Image-guided surgery

Azagury, Dan Elison; Dua, Monica M.; Barrese, James C.; Henderson, Jaimie M.; Buchs, Nicolas C.; Ris, Frédéric; Cloyd, Jordan M.; Martinie, John B; Razzaque, Sharif; Nicolau, Stéphane; Soler, Luc; Marescaux, Jacques; Visser, Brendan C.

How to cite

AZAGURY, Dan Elison et al. Image-guided surgery. In: Current problems in surgery, 2015, vol. 52, n° 12, p. 476–520. doi: 10.1067/j.cpsurg.2015.10.001

This publication URL: https://archive-ouverte.unige.ch//unige:90616
Publication DOI: 10.1067/j.cpsurg.2015.10.001

Current Problems in Surgery 52 (2015) 476–520

Contents lists available at ScienceDirect

Current Problems in Surgery

journal homepage: www.elsevier.com/locate/cpsurg

Image-guided surgery

The neurosurgical origins of image-guided surgery

James C. Barrese, MD, Jaimie M. Henderson, MD

Introduction

The safe and effective practice of surgery requires an intimate knowledge of anatomy. A thorough understanding of surgical anatomy empowers the surgeon to plan a suitable approach, predict possible complications, prepare necessary equipment, and properly counsel the patient. Advances in medical imaging technology have helped surgeons to perform all these tasks by providing more detailed and patient-specific anatomic information before surgery. Surgical precision is especially important for neurosurgical procedures where damage to nearby structures can result in permanent disability or death. Consequently, neurosurgeons have adapted modern imaging techniques for use in the operating room. The integration of stereotactic (coordinate based) systems with advanced imaging and personal computers ultimately led to the development of modern day image-guided surgery. The term image-guided surgery can be broadly defined as any invasive therapy performed with the assistance of, and guided by, images of the treated organ.[1] This general definition includes endoscopy, fluoroscopy, intraoperative computed tomography (CT) or magnetic resonance imaging (MRI), ultrasound, and stereotaxis. Most commonly, however, image-guided surgery refers to stereotactic surgery where preoperative images are registered to the surgical space through the use of reference markers called fiducials and a tracking device in the surgical field displays the surgeon's anatomic position on 3-dimensional (3D) reconstructions of the preoperative films. In this monograph we briefly review the history of stereotactic neurosurgery and the technological breakthroughs that made image-guided surgery possible. We also examine the essential elements of current image guidance systems and discuss neurosurgical applications.

Historical perspectives

Stereotactic neurosurgery refers to a variety of techniques for performing intracranial procedures with a high level of precision and accuracy by establishing a fixed coordinate system within the brain. Traditionally, stereotactic head frames have been used to establish a coordinate system and introduce various instruments such as needles or electrodes. The development of stereotactic frames began toward the end of the 19th century. In 1873, Dittmar used a

http://dx.doi.org/10.1067/j.cpsurg.2015.10.001

stabilization arm to precisely lesion the medulla in rabbits.[2] In 1889, Zernov developed an "encephalometer" to target brain structures based on surface contours of the skull.[3] However, neither of these systems used fixed coordinates. It was neurosurgeon, Sir Victor Horsley, and surgeon/mathematician, Robert Clarke, who first introduced a frame utilizing the Cartesian coordinate system (Fig 1). Horsley and Clarke[5] used their frame for lesioning studies in monkeys, but never adapted it for clinical use in humans.[4] Spiegel and Wycis were the first to successfully adapt the Horsley-Clarke frame for human use in 1947. They used pneumoencephalograms to visualize the anterior commissure of the thalamus and pineal gland (often calcified), which they used as references to establish the coordinate system. Imaging the patient also helped account for the variation between skulls and made the coordinate system more specific to the patient. Spiegel and Wycis called their technique "stereoencephalotomy" and first applied it to psychosurgery by making targeted thalamic lesions. They were striving to find a safer alternative to the destructive frontal lobotomies that were popular at the time.[6,7] During the 1950s, stereotactic neurosurgery was applied to the treatment of movement disorders, pain, and epilepsy. More than 40 different types of frames were developed throughout the 1950s and early 1960s.

The introduction of CT in the 1970s and MRI in the 1980s led to a number of breakthroughs in the field of stereotactic neurosurgery. Neurosurgeon Lars Leksell invented an arc-based stereotactic frame in 1949 that was later adapted for use with CT by Bergström and Greitz in 1976.[8,9] In this system, the Leksell frame was mounted to the CT scanner, making it possible to directly transfer coordinates from the scanner to the frame. Stereotactic targets could now be directly localized with great accuracy, significantly reducing the need for indirect targeting based on a standardized atlas. In 1979, a medical student named Russell Brown designed a fiducial system (the N-localizer) that enabled the transfer of imaging coordinates to frame coordinates without being physically attached to the scanner (Fig 2). This breakthrough made it possible to use any CT or MRI to plan stereotactic operations whereas the previous Leksell system required a specially designed scanner.[10] Brown's invention was adapted for use with

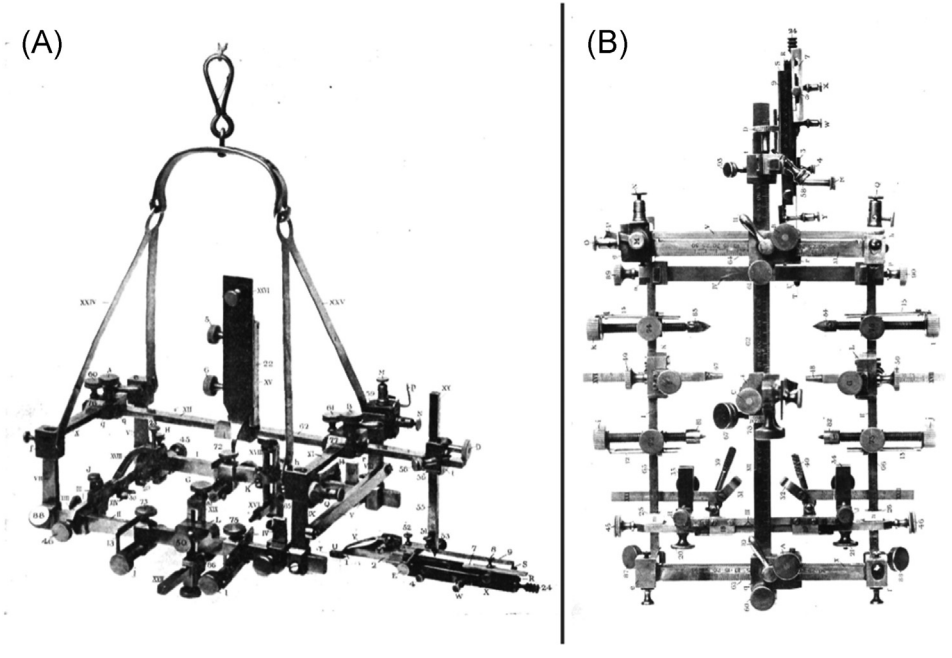

Fig. 1. Horsley-Clarke stereotactic frame. Views from the side (A) and top (B) of the original frame developed by Horsley and Clarke in 1908 for use in animal experiments.

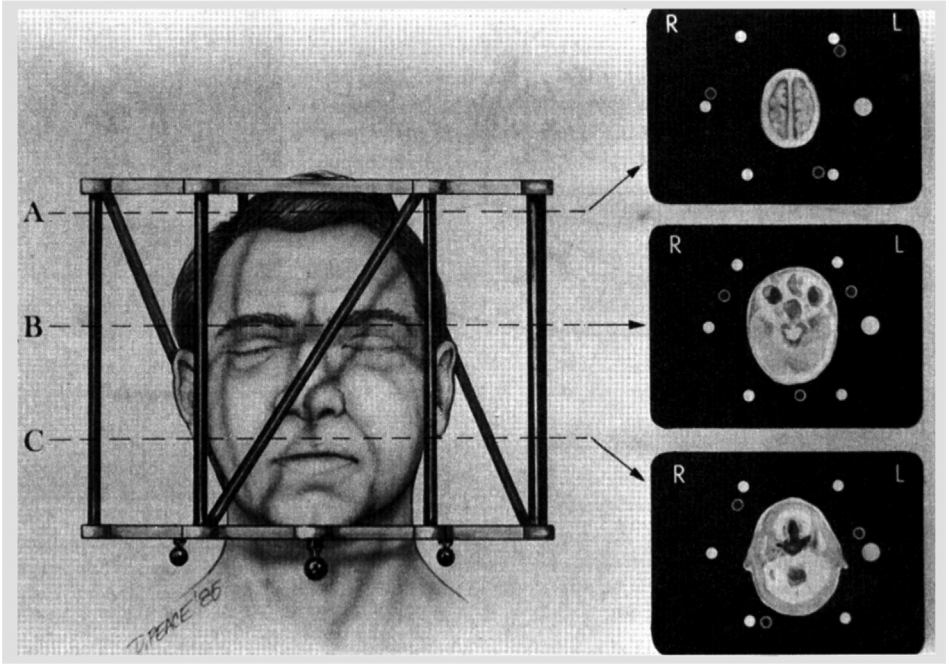

Fig. 2. Russell Brown's N-localizer. The N-localizer ring mounted onto a frame and had 6 vertical posts and 3 diagonal posts. The distance between diagonal and vertical posts was measured on each axial CT image making it possible to determine the *z*-coordinate at any point within the localizer volume.

several frames, including the Cosman-Roberts-Wells frame and Leksell frame, both of which are commonly used today.

In the 1980s computing power increased significantly and image-guided surgery entered the modern era. Computers made it possible to create 3D volumetric reconstructions of CT and MRI images. In 1980, Jacques developed a frame-based system with an arc-mounted micromanipulator that targeted lesions using preoperative 3D reconstructions of tumor volumes. This "volumetric" approach to surgery marked the first time that stereotactic coordinates were defined as a volume rather than a point.[11] Neurosurgeon, Patrick Kelly, adapted this technology to treat tumors with a CO_2 laser in 1982. He outlined the lesion volume on preoperative films and programmed a computer to move the frame-mounted laser to target.[12]

In 1986, David Roberts and John Strohbehn revolutionized image-guided surgery by introducing frameless stereotactic surgery. They accomplished this by first obtaining a CT scan with 3 radiopaque reference markers (fiducials) placed on a patient's scalp. These fiducials were outlined on preoperative images and the surgical target was defined. In the operating room, the patient's head was immobilized and an array of microphones was attached to serve as a fixed reference. The surgical microscope had several spark gaps that generated sound waves picked up by the reference microphones (Fig 3). The transit time of the sound waves was used to determine the position and orientation of the microscope's focal point in space. By using the microscope to register the position of each fiducial, the relationship between CT coordinates and real space coordinates was determined by a computerized transformation matrix. This system also projected the volume of the surgical target (eg, a tumor) into the optics of the microscope (Fig 3). Every time the microscope was moved during surgery, the spark gaps would fire, the microphones would relay timing information to the computer, position would be determined in terms of CT coordinates, and the optical projection would update the target boundary.[13] It took nearly 20 seconds for each update cycle. In 1987, Watanabe and colleagues[15] devised a method to track a surgical probe in real time using an articulated arm fitted with potentiometers.[14]

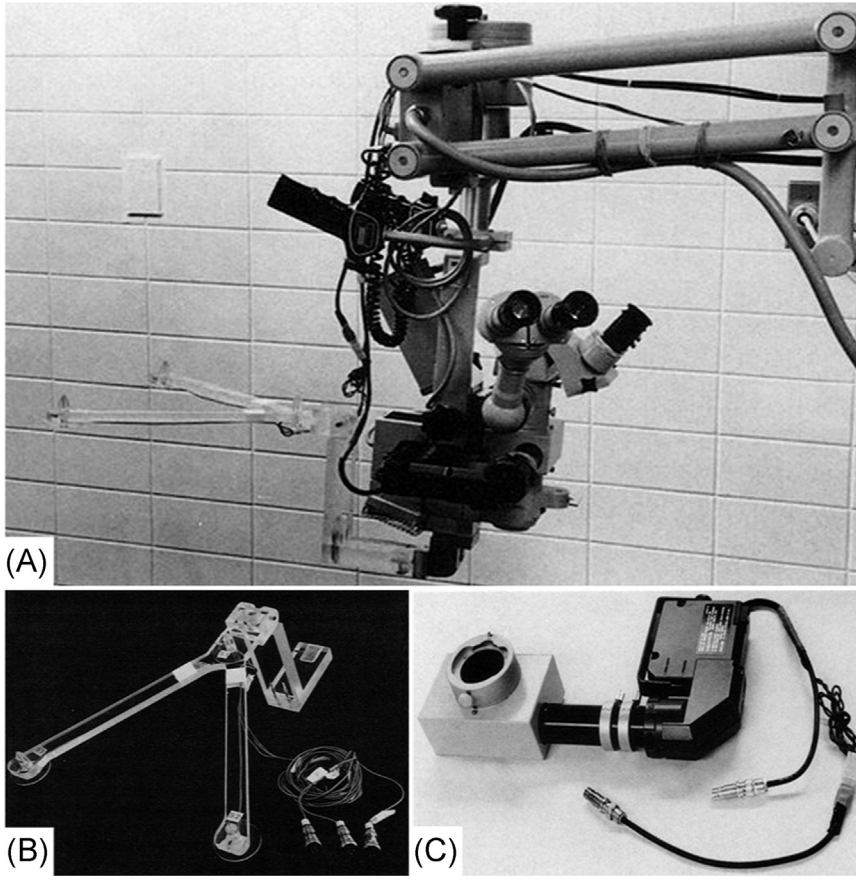

Fig. 3. David Roberts' frameless stereotactic navigation system. (A) Operating microscope with spark gap emitters that are mounted opposite the surgeon's eyepiece. (B) Detail of the 3 spark gaps used for acoustic tracking. (C) The projector system that mounted to the bottom of the microscope and displayed target boundaries to the surgeon.

He could visualize the anatomic location of his probe on preoperative films and although it did not require a microscope, was still quite cumbersome.

In the 1990s, neurosurgeon, Rich Bucholz, was instrumental in developing a frameless navigation system that tracked surgical instruments in real time.[16,17] Bucholz combined the acoustic tracking technology developed by Roberts, the computer vision system developed by Heilbrun and colleagues,[18,19] and the instrument tracking technology of Watanabe. Later improvements in his system included the transition to optical tracking using light-emitting diodes (LEDs), the skull-based screw fiducial system developed by George Allen in 1993,[20,21] and more powerful computers for visualization that displayed probe position in multiple planes. This system was commercialized and after a number of corporate acquisitions and technical upgrades, eventually became the Medtronic StealthStation[17] (Fig 4). Although several other image guidance systems are on the market today, the StealthStation was the first to contain all of the essential elements that define modern day image-guided surgery.

Fundamentals of image-guided surgery

There are several basic elements common to all image guidance systems. These elements include image acquisition, planning, registration, instrument tracking, and visualization.

Fig. 4. Medtronic's S7 StealthStation. The S7 is the most recent model of Medtronic's image-guided surgery platform. On the left is a large high-definition touch-screen monitor. To the right is the navigation computer and planning workstation. Note that the infrared camera used for optical tracking is attached to the workstation and positioned above the surgical field.

Image acquisition is the process of obtaining preoperative imaging studies and loading them into the image guidance software. Image guidance systems generally interface with a hospital's radiology network or permit Digital Imaging and Communications in Medicine (DICOM) formatted images to be loaded with a compact disc (CD) or USB drive. High-resolution CT and MRI images are most commonly used in neurosurgery with a slice thickness ranging from 0.5-2.0 mm. CT and MRI both have advantages depending on the goal of surgery. CT is useful for defining sinus anatomy in endoscopic endonasal procedures and CT angiograms can be helpful for aneurysm surgery. When skull-based titanium fiducials are used, CT is required. CT and MRI scans can be merged using planning software allowing the high accuracy obtained with skull fiducials to be translated to MRI. Contrasted T1 sequences are useful for defining blood vessels and tumors. T2-weighted images show cerebrospinal fluid very well. Multiple different series can be merged and blended to varying degrees. This feature aids in surgical planning (Fig 5). For example, before implanting a deep brain stimulator, the combination of MRI sequences allows the surgeon to target lead placement on T2 images and plan a lead trajectory devoid of blood vessels on the contrasted T1 images. More specialized sequences are used to display white-matter fiber tracts and can help the surgeon avoid damage to eloquent brain areas during tumor resections. Most planning software packages can generate 3D reconstructions, overlay standardized anatomic atlases (Fig 5), and define a trajectory with preselected target and entry points.

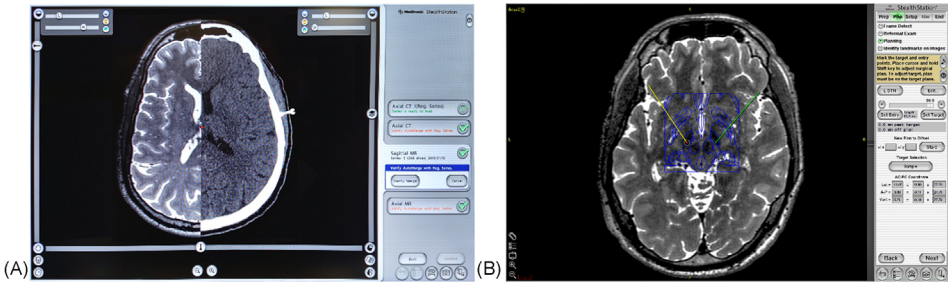

Fig. 5. Planning software. (A) This screenshot from the StealthStation planning software shows a reformatted sagittal T2 MRI being merged with an axial CT scan. *Note*: the skull screw on the CT that serves as a fiducial marker for registration. (B) The second screenshot shows an axial T2 MRI superimposed with a stereotactic atlas. This aids in planning electrode placement during deep brain stimulation.

Registration is the process of creating and linking coordinate systems in real space (the operating room) and digital space (the volumetric reconstruction of imaging data). This can be accomplished using preselected points or surface topography. Point merge systems require selecting points on preoperative images (fiducial or anatomic landmark) and then communicating where those points are in real space to the computer through optical tracking technology (Fig 6). A camera placed above the surgical field emits infrared waves and senses the reflection off passive markers on a reference fixed to the patient's headframe or skull. A mobile probe with reflective markers is used to inform the camera and computer where the fiducials are in relation to the reference frame (Fig 7). Once the location of each fiducial has been sent to the computer, a transformation matrix is applied. An alternative to point merge is facial topography. In this system a patient's face is scanned with a handheld laser or traced with an optical probe allowing

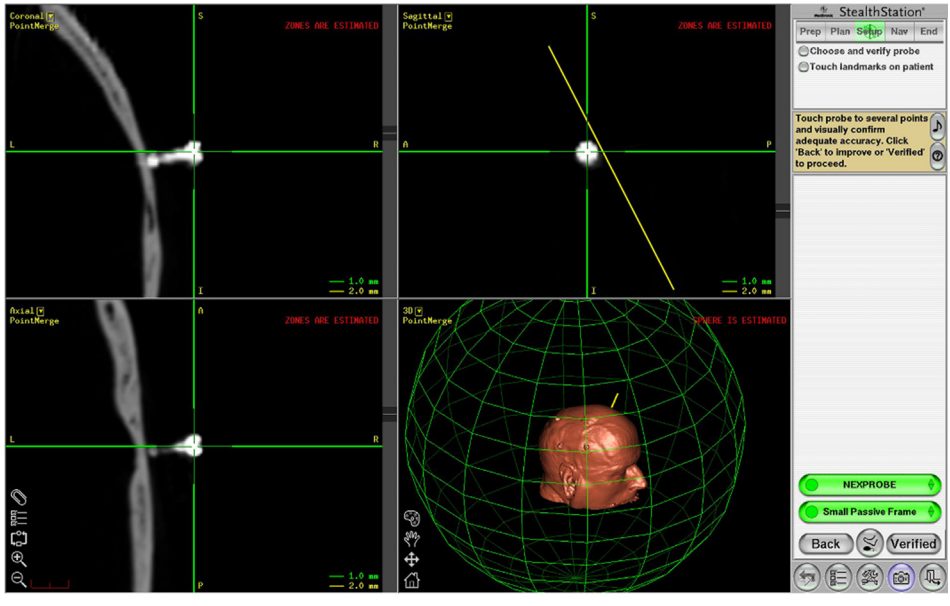

Fig. 6. Point-merge registration. During planning, the center of each skull-based fiducial (metal screw) is selected by the surgeon and stored in the computer. During registration, the tip of an optical tracking probe is placed into the center of each fiducial screw. The computer will then apply a transformation matrix to align the 3D model to the surgical field. *Note*: the green sphere surrounding the model of the patient. This indicates that there is less than 1 mm of error while tracking within the volume of the sphere.

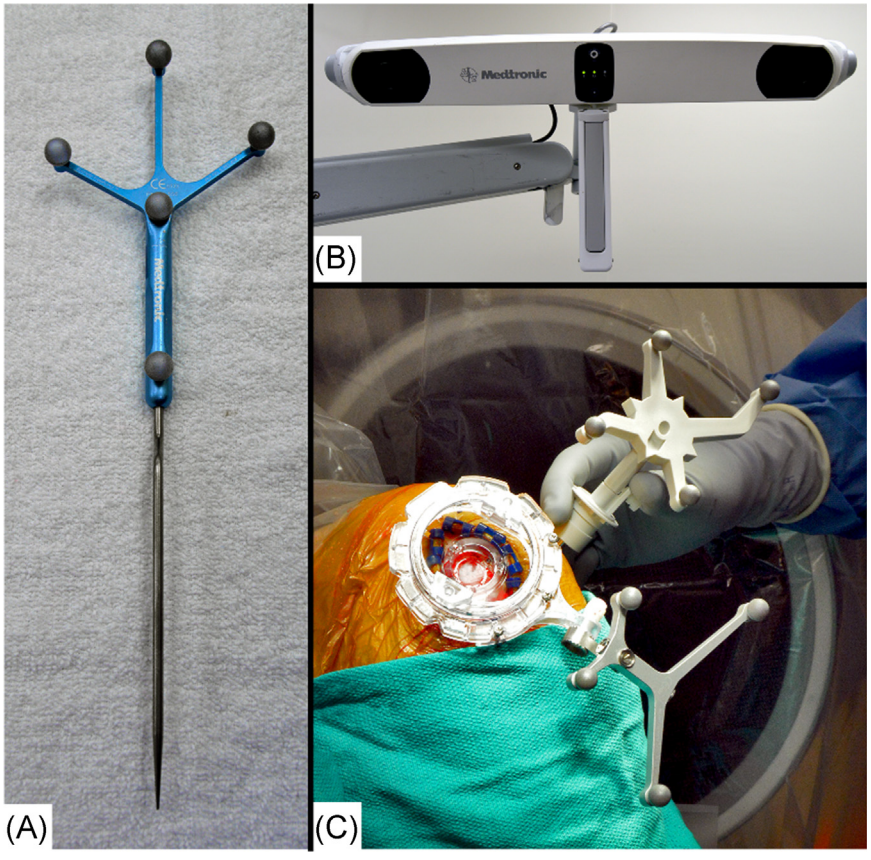

Fig. 7. Tracking instruments. (A) A typical optical tracking probe. Note the reflective spheres that relay position information to the infrared camera. (B) The camera that both emits and receives infrared waves. It is positioned above the surgical field and must maintain line-of-sight with the reference frame and tracking probe. (C) This photo illustrates a skull mounted reference frame and another optical tracking probe. The reference frame is fixed to the patient's skull, but the tracking probe can be moved around the field. The position of the probe in digital space is determined based on its relative position to the reference frame once registration is complete. The instruments shown in this figure are the Nexframe and Nexprobe, which are used for placement of deep brain stimulator electrodes.

the computer to apply a transformation matrix based on topography[22] (Fig 8). This is a much faster and easier method but not as accurate as the point merge system.

Localization and real-time tracking of a surgical probe or instrument can be accomplished using a variety of methods. As previously mentioned, this can be accomplished with sound waves,[13] infrared light,[17,23,24] or other technologies. One method that is becoming more widely adopted involves electromagnetic fields. Instead of using a microphone or camera to determine probe position, a magnetic coil is used to track a probe. In this system, the probe uses electricity to generate perturbations in the magnetic field generated by the reference. One advantage of this system is that line-of-sight does not need to be maintained while tracking.[25] Once a patient is registered and instruments are ready for tracking, the surgeon must have a way to visualize his anatomic location. Image guidance systems use a high-definition monitor to display position to the surgeon. Traditional views such as axial, coronal, and sagittal are standard features. More advanced tools are also available, depending on the manufacturer. The StealthStation, for example, offers 3D reconstruction, fiber tracking, guidance view, trajectory view, and stereotactic atlas overlay. Guidance view projects the target as a circle in the center of a crosshairs and

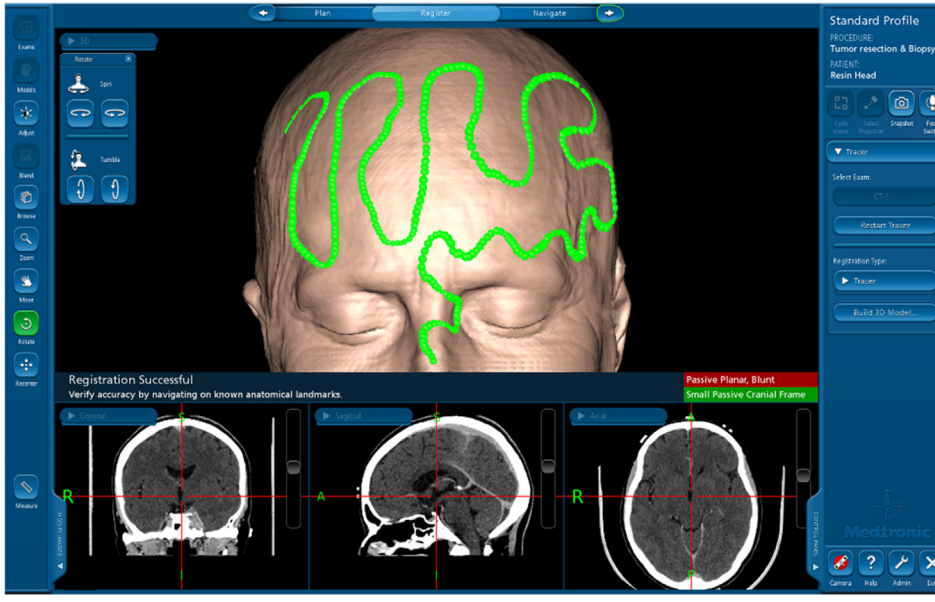

Fig. 8. Facial tracer registration. Facial topography can also be used to register a patient for image guidance. A tracking probe is traced along the contours of the face while the computer records the position of the probe's tip. A transformation matrix is applied to all of these points in order to establish the coordinate system. This screenshot shows a typical pattern surgeons use when tracing facial topography.

the current trajectory as a point that must be kept within those crosshairs (Fig 9). This is especially useful for stereotactic procedures where an electrode or biopsy needle is being introduced into the brain.

Current applications and the future of image-guided surgery

Having evolved from stereotactic neurosurgery, image-guided surgery is routinely used for placing depth electrodes, biopsy needles, and instruments for ablative procedures. The use of image guidance in tumor surgery has also become routine because the boundary between tumor and normal brain is often difficult to distinguish with the naked eye. The increasing demand for minimally invasive surgery has led to many innovations that utilize image guidance. The most well known example is perhaps radiosurgery. Neurosurgeon, Lars Leksell,[26] first applied stereotactic principles to radiation therapy and he helped develop the Gamma Knife in the 1960s. The linear particle accelerator, or Linac was developed in the 1980s and neurosurgeon, John Adler,[27] built upon this technology in the 1990s when he developed the CyberKnife. Another minimally invasive technique is MR-guided laser interstitial thermal therapy. This thermal ablation technique is done by stereotactic placement of a laser catheter followed by real-time MR thermography to monitor the extent of the ablation.[28] laser interstitial thermal therapy was originally designed to treat tumors but has been successfully applied to the treatment of temporal lobe epilepsy by performing amygdalohippocampal ablations.[29] Spine surgeons and orthopedic surgeons are now placing instrumentation using image guidance.[30,31] Neurosurgeons and otolaryngologists have developed image guidance systems for tracking endoscopic instruments during endonasal procedures.[32] General surgeons have pioneered the use of ultrasound to track soft organs during surgery, a technology that has tremendous potential for solving the problem of “brain-shift” in neurosurgery.[33-37] As technology rapidly evolves, and more surgical specialties find innovative ways to use image-guided surgery, we will continue to make surgery safer and less painful for our patients.

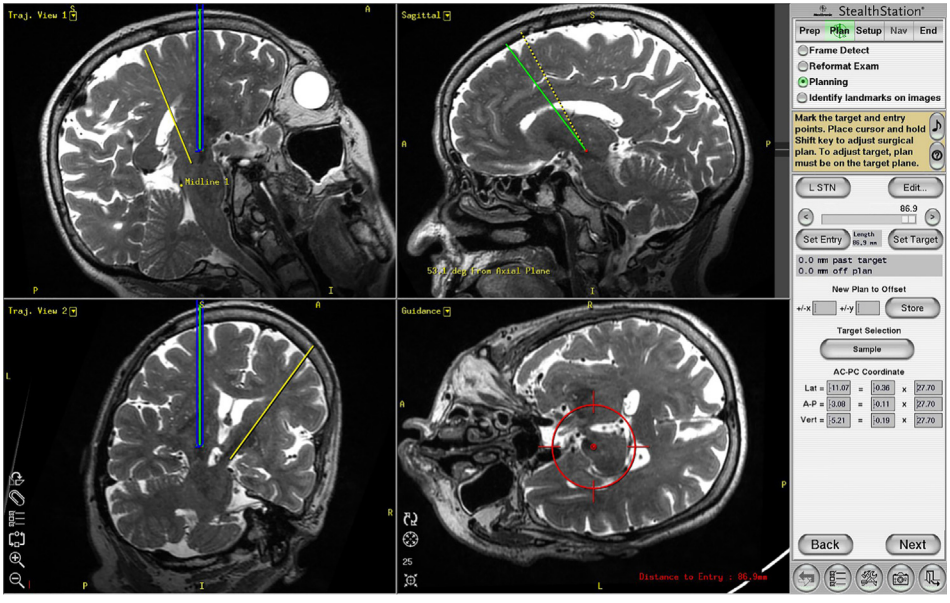

Fig. 9. Visualization. There are a variety of options for visualization during surgery. The StealthStation provides trajectory views, which are helpful when placing needles or electrodes. The images are reformatted and displayed in oblique cuts that are in the plane of the planned trajectory (top-left and bottom-left quadrants). This allows the surgeon to see all of the structures that will be encountered by an instrument as it is passed through the brain. Guidance view is especially helpful when lining up an instrument before passing it into the brain. The bottom-right quadrant shows crosshairs that indicate the expected trajectory and a circle in the center representing the target. By keeping the target in the center of the crosshairs, the surgeon can be sure that his instrument is advancing along the planned trajectory. The top-right quadrant shows a standard sagittal view.

Ultrasound-based advanced guidance systems for abdominal surgery

John B. Martinie, MD, Sharif Razzaque, PhD

Background

The use of ultrasound as we know it in medicine was pioneered in the 1930s and 1940s. Karl Dussik, an Austrian neurologist, is generally regarded as the first to use ultrasound in a diagnostic role in medicine, when in the 1930s, he proposed using this technology to evaluate the ventricular system of the brain and to detect brain tumors. His original “hyperphonograms” with central density corresponding to the ventricular system were limited by poor transmission though the bone of the calvarium. In the 1940s, ultrasound was first described in a role in which it remains clinically current; US Naval physicians George Ludwig and Francis Struthers described the use of ultrasound to detect foreign bodies when they implanted extracted human gallstones in the gallbladders of dogs and later detected and characterized them with ultrasound. In their 1949 report detailing the soundwave frequency needed to penetrate different human tissues, the authors concluded that ultrasound could be employed “for the detection of tumors and foreign bodies other than gallstones,” underscoring the future potential of this technology in the field of diagnostics. The characteristic 2-dimensional (2D) grey-scale image of B-mode (brightness mode) ultrasonography was developed later, when a pair of developments in the 1950s and 1960s allowed for real-time evaluation of tissues of differing densities. Since that time, further advances in ultrasonography, include the application of the Doppler effect to evaluate blood flow, therapeutic ultrasound, and the integration of ultrasound into the operating room to guide surgical therapy and decision making.

Ultrasonography is based on the passage of focused sound waves into tissue and the reflection of these back to the transducer where the change in frequency and intensity of the reflected sound is interpreted and used to form an image. Electricity from the ultrasound device is passed into the transducer, the portion of the apparatus that is placed in contact with tissue. Uninterrupted tissue interface, typically facilitated with a water-soluble gel, is critical in ultrasonography because sound waves, unlike other forms of transmitted energy, is inefficiently transmitted through air. When the electrical signal reaches the transducer it causes vibration of the piezoelectric element, the component of the ultrasound machine that creates the high frequency sound waves that emanate from the transducer and are directed into tissue. As these sound waves contact tissues of varying density, a portion known as the echo pulse is reflected back to the transducer where a second piezoelectric element is caused to vibrate by the returning sound waves; this vibration is converted to an electric signal that is processed into an image representing the densities of the tissues that reflect the ultrasonographic waves.

The piezoelectric effect employed for sound wave generation in ultrasonography is based on a late 19th century discovery that certain substances produce an electric charge when a mechanical force is applied to the substance resulting in vibration. The produced sound waves used in diagnostic ultrasonography range in frequency from 2-20 MHz or 2-20 million cycles per second. The images seen during the use of B-mode ultrasonography are based on tissue density, the angle at which the beam and tissue interface; the amount of time required for the return of the transmitted waves is used to determine distance or depth from the transducer. The frequency of generated sound is determined by the piezoelectric element in the transducer. These were originally crystals but ceramic compounds have also been developed. The frequency of sound generated by the crystal is an innate property of the crystal, meaning that waves of different frequencies require the use of different transducers. This has led to the adoption of certain wavelengths and transducers for specific regions of the body or organs to be evaluated, typically based on depth and location of the area of interest. High frequency waves produce more reflection from tissues per unit time, resulting in a higher resolution image. Owing to this, the depth of tissue penetration is limited, requiring lower frequency waves to evaluate deeper structures.

The image produced by ultrasound is dependent on the sound waves' interaction with tissue and the reflection of sound waves off of tissues back to the transducer. The waves' motion through tissue is degraded over time by transfer of energy to tissue, creating heat. This loss of energy, by any means of energy transfer, is referred to as the attenuation of the pulse. Specific tissues (liver, adipose, and serous fluid) have calculated values that describe their attenuation of the pulse energy; the higher the attenuation coefficient of a tissue, less of an ultrasound pulse is able to penetrate. On this spectrum, serous fluid degrades the energy of a pulse the least while bone is not penetrated to absorption of energy. Other factors that attenuate a pulse amplitude include the reflection that occurs at interfaces of tissues of differing levels of resistance to the transmission of sound waves, known as acoustic impedance. At tissue interfaces, a portion of the pulse is reflected toward the transducer whereas some of the pulse continues into the abutting tissue. The difference in the impedance to sound transmission determines the amount reflected to the transducer and consequently the definition of the interface seen on the ultrasound display.

Given the detailed physical properties of ultrasound and their interaction with tissue, use of ultrasonography in surgery requires proficiency with orientation of the transducer and interpretation of images based on spatial orientation and a detailed knowledge of the surrounding anatomy. Despite an initial learning curve in obtaining and interpreting ultrasound images, the advent of B-mode ultrasonography and Doppler images has fostered the adoption of this dynamic, real-time imaging modality in multiple fields of surgery. Ultrasound has led to paradigm-altering changes in the evaluation of carotid artery disease, abdominal aortic aneurysms, and blunt abdominal trauma.

Ultrasound has many capabilities but is usually thought of as quite simplistic compared to other imaging modalities, such as CT, MRI, or positron emission tomography. The images, at least in older systems, are often 2D, black and white, fuzzy and indistinct shadows that can be as

challenging for the surgeon to interpret as modern abstract paintings. The spatial and 3D anatomy of cross-sectional imaging modalities such as CT and MRI lend themselves to much easier interpretation for most physicians, who not surprisingly, tend to utilize those modalities more frequently. With the phenomenal growth in the utilization of CT and MRI over the past 20 years, as well as improvements in resolution and image quality, it seems as though ultrasound was abandoned by many physicians. Indeed, "why would one order an ultrasound, when you can get so much more information from a good CT scan?" Yet ultrasound systems have quietly and steadily improved in terms of image quality, clarity, resolution, and ease of use of the actual hardware and operating systems. There are now several systems (BK Medical and Aloka) that are designed specifically for surgeons to use in the operating room, obviating the need to call a radiologist to the room. These systems are much smaller, more streamlined, and simpler to use than many of the larger ultrasound systems designed specifically for diagnostic radiologists or obstetricians. Truly portable systems (Sonosite), designed for trauma evaluation or vascular access guidance, are now ubiquitous tools in emergency departments everywhere in the United States, and even part of military combat medical teams. There are even ultrasound systems that can be attached to smartphones.[38]

Yet ultrasound requires training to operate the actual systems and control panels, to handle the transducers, and to interpret the ultrasound images. This training simply did not exist in most surgical training programs until recently and expectedly, most surgeons lacked the skills to use ultrasound. It was not until the late 1990s that surgical residencies began incorporating ultrasound into training, and this came about largely due to the emergence of the focused assessment with sonography for trauma (FAST) exam for abdominal trauma.[39,40] Formal training in ultrasound is now a mandatory requirement for general surgical residencies in the United States, and this training includes the use of ultrasound for abdominal and thoracic trauma, thyroid and neck masses, breast lumps, and evaluation for gallbladder pathology. In many of these instances, ultrasound provides quick, inexpensive, noninvasive, and easy to interpret information to guide the physician in real-time urgent scenarios.

Perhaps, nowhere else in abdominal surgery is precise image guidance as important as it is in the fields of liver and pancreatic surgery. Indeed, the emergence of surgical ablation (radiofrequency ablation [RFA]) in the 1990s as a therapeutic tool for the management of hepatic serves as one of the best examples where imaging and guidance are critical to the success of the actual treatment. At the time when surgeons first began using RFA in the operating room, many did not possess the requisite skills to perform accurate targeting of the intrahepatic tumors. Inaccuracy, no doubt, led to higher rates of incomplete ablations, which in turn, were interpreted as "local recurrences." Many early reports of RFA unfortunately garnered a reputation for the modality as inadequate with local recurrence rates of up to 30%, a rate that is quoted by many surgeons to date.[41,42] And as is often the case, the surgeons blame to tool, or the instrument, or the device as the problem, as the reason for failure. And although it certainly is true that many of the early RFA systems had technical shortcomings, more than 20 years of constant development and improvement have largely eliminated the glitches. Modern reports of both RFA and microwave ablation from high volume center have reported excellent results with local recurrence rates of under 3%.[43,44] The common theme for obtaining these results seems to be volume and experience with not only the ablation systems, but with ultrasound guidance. Indeed, many of the high volume centers that perform hepatic tumor ablation are also centers involved in teaching ultrasound courses and research in ultrasound guidance technologies.

Basic ultrasound guidance

Ultrasound is an incredibly useful, low-cost, noninvasive imaging technology that allows the operator to locate pertinent anatomical landmarks in the body for accurate targeting. It has been used in a multitude of surgical procedures, including tumor ablation, central line placement, soft tissue biopsies (breast, thyroid, and lymph node), and thoracentesis and paracentesis. There is a

growing body of data to support the use of ultrasound in these and other procedures to reduce errors and improve safety and outcomes.[45,46] Yet for many, acquiring these ultrasound skills is not immediately inherent. For more complex procedures, such as a laparoscopic microwave ablation of a liver tumor using a flexible ultrasound probe, there are so many different angles and trajectories involved that this procedure can prove impossible even for expert liver surgeons. The biopsy needles and ablation antennae are extremely thin and difficult to visualize using traditional 2D ultrasound. The idea of having a system that would allow for a "GPS" or "navigation" so that the needle could be placed precisely the first time, every time gave rise to the field of "tracked ultrasound" guidance systems.

Ultrasound-based advanced guidance

An "advanced guidance system" or "navigation system" is one that contains both an imaging modality (in this case, ultrasound), as well as a means by which to *track* or localize surgical instruments in space. There are several critical elements in all of these systems, but none of them are more important than the actual computer, both hardware and software, which handles and incorporates information from the various components and exports the fused images to a video monitor. Initial systems purportedly required computers the size of living rooms, although current systems typically run off of commercially available laptop computers. The actual "tracking system" is the means by which location and spatial orientation data is registered and relayed back to the computer. Early tracking systems consisted of mechanical arms or calipers that provided a physical connection between the ultrasound transducer and a fixed point so that the computer would know precisely where the ultrasound image should be placed relative to the end organ or surgical instrument (Fig 10). As the surgeon moved the ultrasound hand-piece, the angles and position of the mechanical arm change, and these data were relayed to the computer, allowing the system to pinpoint the precise location and orientation of the ultrasound image. These early systems, although certainly functional, presented practical and logistical barriers to their adoption in the operating room in sterile environments. Researchers looked for ways to "break the chains" and physically disconnect the ultrasound probe and other surgical instruments from the tracking device and the mechanical arms. The 2 subsequent types of systems are optical tracking systems (OTSs) and electromagnetic tracking systems (EM or EMTSs). A comprehensive study of these systems is beyond the scope of this chapter, but it is important to understand the basic concepts in order to grasp the concept of "navigation" and "tracked ultrasound."

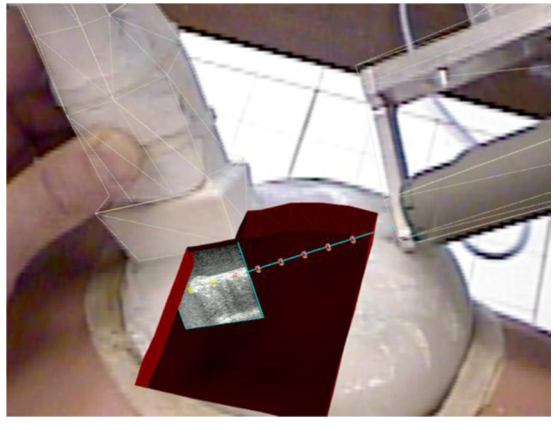

Fig. 10. This breast ultrasound model demonstrates an early tracking systems consisting of a mechanical arm that provides a physical connection between the ultrasound transducer and a fixed point on the breast tissue.

2D vs 3D ultrasound

Much of the research that has been done on ultrasound-based guidance systems focuses not only on the actual navigation or tracking components, but also the differences between standard 2D and enhanced 3D ultrasound. As mentioned earlier, one of the limitations of standard ultrasound is that it represents visually only a thin slice of the target anatomy at any given time, although it is constantly refreshed, while 3D ultrasound "captures" a "volume" of ultrasound data over time.[47]

Optical tracking systems

The original OTSs consisted of LEDs (light-emitting diodes) positioned on the handles of surgical instruments or ultrasound hand pieces, and sensitive cameras located above the operative field. By detecting the spatial position and orientation of a cluster of LEDs by multiple cameras, the system can triangulate the location and orientation of the instrument to which those LEDs are attached. The concept is not unlike the way modern cell phones can provide positional information by using cell phone towers to triangulate their position. Subsequent generations of OTSs replaced the LEDs (active systems) with reflective spheres and infrared emitters/cameras (passive systems), which eliminated the need for wires being attached to the instruments **(**Fig 11**)** The use of these systems has been described by many groups, in a variety of applications, for neurosurgical procedures and abdominal operations. An early study at the University of Trondheim, Norway demonstrated the feasibility of using an OTS to perform targeting of phantom tumors in ex vivo calf livers (in an open fashion) and demonstrated superiority in both ease and accuracy with the navigation system.[48] They also compared 2D and

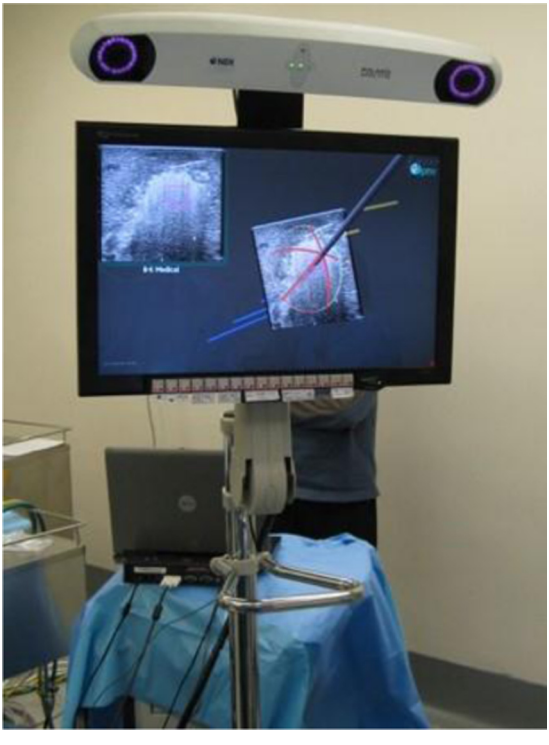

Fig. 11. Intraoperative photograph of an optical tracking system camera and monitor.

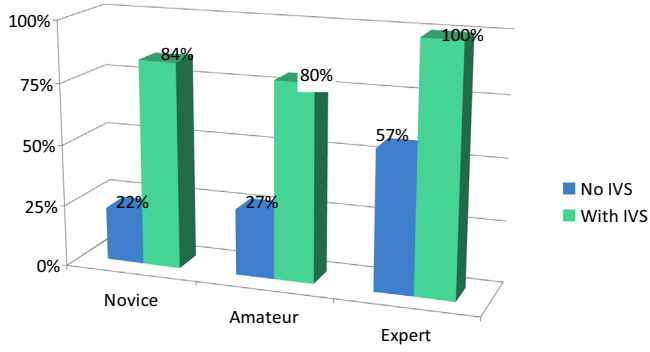

Fig. 12. Outcomes of using an ultrasound navigation system with 2D ultrasound to target 5 mm phantom tumors in gelatin agar models. Overall, 3 skill level users performed multiple attempts with and without the guidance system. Accuracy = % of first time direct hits of 5 mm target. $n = 60$ per skill level. $P < 0.0001$ for each level. (Color version of figure is available online.)

3D ultrasound and found that motion of the target tissue or phantoms following 3D image acquisition limited the accuracy of the system.[48] Our group at Carolinas Medical Center described a similar 2D ultrasound-based OTS for open targeting phantom liver tumors ex vivo and were able to demonstrate statistically significant improvement in accuracy for all skill level operators (Fig 12). By eliminating the use of 3D ultrasound, the image acquisition phase was also simplified, and errors due to movement of the target anatomy were eliminated. A pilot trial was then performed using this 2D ultrasound-based OTS (Invision system, Inneroptic, Hillsboro, NC) to assist with open liver tumor ablation in human patients.[37] A total of 31 tumors in 8 patients were ablated by liver surgeons experienced in both ultrasound and ablation. All lesions were targeted in a single pass, as determined by an independent radiologist observer, again validating the ease and accuracy of these systems.[37] Subsequent groups have validated the use of ultrasound-based OTS, predominantly on open, ex vivo studies.

One of the earliest descriptions of a prototype laparoscopic, ultrasound-guided ablation systems was described by the group at Vanderbilt, utilizing LEDs on the instruments and a rigid ultrasound probe to acquire 3D ultrasound images.[49] They were able to demonstrate both feasibility and proof of concept and may represent the very first minimally invasive ultrasound-based navigation systems, albeit in an inanimate, laboratory setting.[49]

During this time period of 2000-2015, there were numerous groups simultaneously developing navigation systems, and there was a trend to migrate from OTSs to electromagnetic tracking systems (EMTSs). And although the OTSs worked well for guiding navigation in the laboratory setting on open phantom models, there were several drawbacks, most notably “line-of-sight” issues. The optical reflectors on the ultrasound hand-piece and surgical instruments had to remain visible to the infrared cameras during the procedure or the navigation would be lost. Moreover, a growing number of surgeons began using laparoscopic approaches to liver and pancreatic surgery, necessitating the need a navigation system that would work with that approach.

Electromagnetic tracking systems

The renewed interest in using electromagnetic tracking systems eliminated the line-of-sight issues, as the coils can be placed within the tips of a flexible ultrasound probe or surgical instruments (Fig 13). The EMTS work by having the patient or target organ placed within a magnetic field that is produced by a magnetic field generator.[50] These devices are now commercially available and can be placed beside, or directly underneath a patient in the operating room. Small sensor coils, when placed within this field, produce a small electrical current when they are moved or change position and orientation.[51] That small current is then transmitted to the computer allowing the system to then locate the precise location and

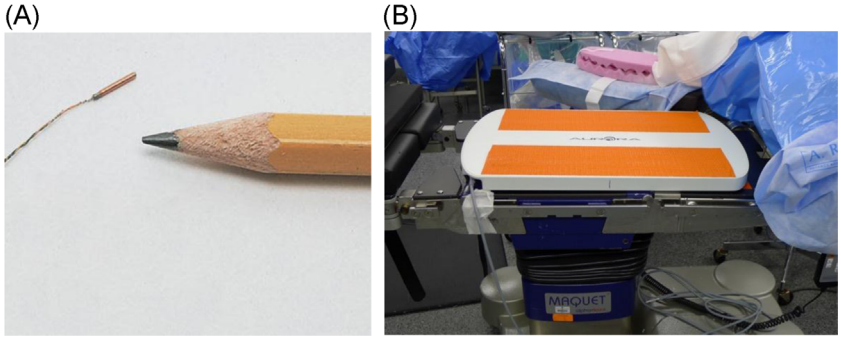

Fig. 13. Electromagnetic tracking system (A) sensor coil and (B) field generator.

orientation of not only the coil, but also the surgical instrument within that coil is placed. Kleeman and colleagues[52] similarly studied a laparoscopic ultrasound based, EMTS in which the magnetic coil sensors were attached to the end of a laparoscopic ultrasound probe, and the resultant images were then projected onto the surface of the liver. The study, published in 2006, provided a glimpse of what was possible, but was limited by the sheer size of the sensors, ($8 \times 8 \times 6\ mm^3$ in size), which was simply too large to be placed inside of surgical instruments of ablation antennae.[52] Konishi and colleagues[53] described an ultrasound-based navigation system that remarkably incorporated both an optical system OTS and an electromagnetic (EM) system for laparoscopic targeting of liver tumors in a porcine model. They were able to demonstrate improved accuracy using the navigation system, and was perhaps the first application using a flexible ultrasound probe in a live animal model. Lango and colleagues,[54] again from the group at the University of Trondheim, performed a thorough review of subject of ultrasound-based laparoscopic navigation systems (both OTS and EMTS) and identified 18 key research papers emanating from 11 centers devoted to research and development in ultrasound-based navigational systems. This article represents the most comprehensive and authoritative summary on the field of ultrasound-based navigational systems specifically designed for laparoscopic abdominal surgery.[54]

Most, if not all, of the studies included in this review were in laboratory settings in ex vivo or in vivo animal models, and there was no evidence for actual use in humans in a clinical trial. Following on our initial work using an ultrasound-based OTS for open liver tumor ablations in a human trial, we sought to develop a minimally invasive system using an EMTS. The system employed a flat electromagnetic generator that is placed beneath the padding of the operating table, under the patient (NDI, Ontario), as well as minute sensor coils attached to the flexible ultrasound probe (BK Medical) and microwave ablation antennae (Angiodynamics). These components were connected to the actual navigation system developed in conjunction with our lab and Inneroptic (Hillsboro, NC), consisting of a portable laptop computer and software, as well as a single high-resolution 3D video monitor. All of the various components are portable, relatively inexpensive, and can be set up quickly in an actual operating room. Initial results using 5 mm phantom targets in agar and various skill levels of operators, there was consistent and remarkable improvement in accuracy using the EM navigation system in a laparoscopic model[55] (Fig 14). A follow-up study was then performed in humans using the same system to perform a series of laparoscopic microwave ablations. There were 45 ablations performed on 34 tumors in 13 patients, the median number of lesions per patient was 2, and the median lesion size was 1.7 cm.[56] The success rate of first-attempt central targeting was 93%; 3 lesions required 2 passes each, and targeting was independently verified by a radiologist reviewing preoperative CTs or MRIs as well as ultrasound images from the procedure.[56] The subjective ease with which the tumors were targeted were also scored, something quite unique in the literature, and again the results were promising. Of all, 9 of the tumors were surface lesions and considered too easy for

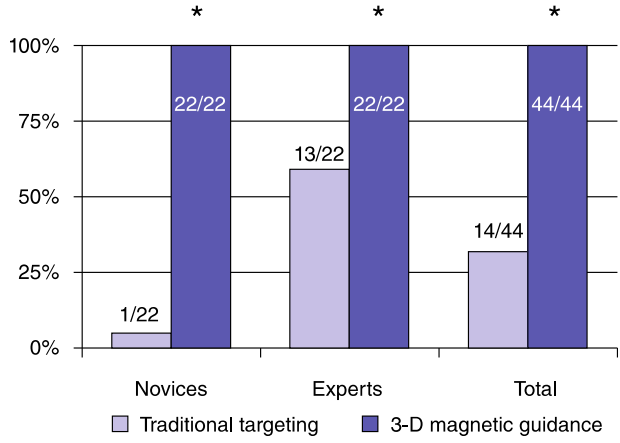

Fig. 14. Surgical novices were essentially unable to hit any of the 5 mm targets using conventional laparoscopy and ultrasound techniques. Expert surgeons had a markedly better ability to target small lesions using traditional technology. Novices as well as expert surgeons succeeded in hitting all targets using the novel magnetic 3D image guidance system. (Color version of figure is available online.)

the scoring evaluation, and 31 of 36 lesions targeted with the systems were scored as very easy or easy. This represented the first time an ultrasound-based navigational guidance system was used in actual human patients in the clinical setting to perform a minimally invasive liver procedure. Although the system and the various components are Food and Drug Administration approved for use, a completely available, “off the shelf” product has yet to come to market.

Image-guided liver surgery

Jordan M. Cloyd, MD, Monica M. Dua, MD, Brendan C. Visser, MD

Introduction

Major hepatectomy is increasingly being performed for a variety of indications.[57] Along with improvements in anesthesia, perioperative medicine, and medical devices, safe complex liver surgery has developed based on a more complete understanding of the segmental anatomy of the liver. Nevertheless, the liver is naturally a solid organ and therefore the intrahepatic location of major vascular and biliary structures can only partially be predicted based on external landmarks. Although advances in computed tomography (CT) and magnetic resonance imaging (MRI) technology have permitted detailed 3-dimensional (3D) mapping of preoperative liver anatomy and pathology, these modalities do not provide dynamic, real time, image guidance during surgery.

Image guidance offers several theoretical advantages to the field of liver surgery: (1) increasing the number of R0 resections and minimizing damage to nearby normal tissue, (2) preserving maximum future liver remnant volume, and (3) planning the division of major vascular and biliary structures may enable less intraoperative blood loss. A successful image guidance platform should satisfy several tenets. First, it should assist in forming a well-designed surgical plan that accomplishes removal of all disease with negative margins and adequate future liver volume. Second, it should permit accurate registration that corresponds to the individual patient in the intraoperative positioning. Finally, it should allow real-time tracking in order to permit true navigation. A perfect platform would be used to overcome human deficiencies, for example, in hand-eye coordination and dexterity.

Fig. 15. Intraoperative photograph of the Pathfinder system demonstrating registration of the preoperative imaging set through a handheld surface probe.

Compared to its use in neurosurgery, the adoption of image guidance in liver surgery has been relatively slow. Several features unique to hepatobiliary surgery present challenges that may explain this fact. The liver does not have the benefit of a fixed reference frame that neurosurgery has (ie, the skull). The liver is subject to deformation during surgery and any real time navigation system must account for motion during respiration. Despite these limitations, there has been tremendous growth in the number of scientific publications on the topic.[58] Nevertheless, the application of image-guided liver surgery in routine clinical practice has been limited. The concept of image-guided liver surgery was most notably introduced by researchers from Vanderbilt and Washington University in 1999.[33] Since then, 2 image guidance systems have been developed and approved for clinical use in the United States whereas many other programs are in development.

Current systems

Pathfinder

Pathfinder Therapuetics Inc (PTI; Nashville, TN) developed the first navigated abdominal surgery platform that is Food and Drug Administration approved for intraoperative soft tissue tracking (Fig 15). PTIs Scout is a useful computer-assisted operation planning tool that reconstructs preoperative cross-sectional imaging (eg, CT or MRI) into 3D reformats. Detailed vascular and biliary anatomy may then be analyzed in relation to specific tumor locations. A planned surgical resection can be simulated and 3D volumetry calculated. Scout works in conjunction with Explorer, PTIs real-time navigation system. Explorer uses a handheld surface probe to register the patient's anatomy with the preoperative imaging set. Alternatively, a laser surface scanner or specialized ultrasound probe may be used for image integration. The system then allows real-time tracking during surgery by mapping various instruments, such as an electrocautery unit or ablation needle.

CAScination

More recently, CAScination AG (Bern, Switzerland) has developed their own fully integrated image guidance platform, CAS-ONE, for liver surgery (Fig 16). CAScination uses MeVis virtual planning software (MeVis Medical Solutions; Bremen, Germany) for 3D reconstruction, liver segmentation, volumetry, and surgical simulation. In the operating room, the image sets are registered to the physical space using distinct surface landmarks. In addition, CAScination's Ubersound integrates real time 3D ultrasound for co-registration. After registration, image guidance is enabled via tracking of any surgical instrument.

Fig. 16. The CAS-ONE Vario system for liver surgery.

Computer-assisted operation planning

The most basic form of image-guided liver surgery is computer-assisted operation planning.[59] This involves image-based volumetry to ensure adequate future liver remnant volume following planned liver resection. This type of analysis has been made possible by significant advancements in cross-sectional imaging as well as advanced surgical planning software. Both CT and MRI have their advantages and may be useful for volumetry. MRI offers excellent soft tissue discrimination but is limited by the speed of acquisition and blurring due to motion. On the other hand, multislice helical CT can be performed in a single breath-hold, allowing pristine images without blur. Contrast enhancement easily delineates arterial, portal venous and hepatic venous structure. The most commonly utilized commercial software is the MeVis Distant Services (MDS) virtual liver planning system (Fig 17). Other software systems are available, such as OVA (Hitachi Medical Corporation, Japan), Virtual Place (AZE, Japan), mint Liver (Heidelburg, Germany), and VR-Render (IRCAD, France), among others.

Computer-assisted operation planning basically permits virtual hepatectomy based on individual anatomic and tumoral constraints, providing information on the optimal operation and the planned FLR (future liver remnant) (Fig 18). Regardless of the software utilized, computer-assisted operation planning involves multiple steps. First, preoperative liver images (CT or MRI) are uploaded to the 3D image-processing software. Second, 3D reconstruction is

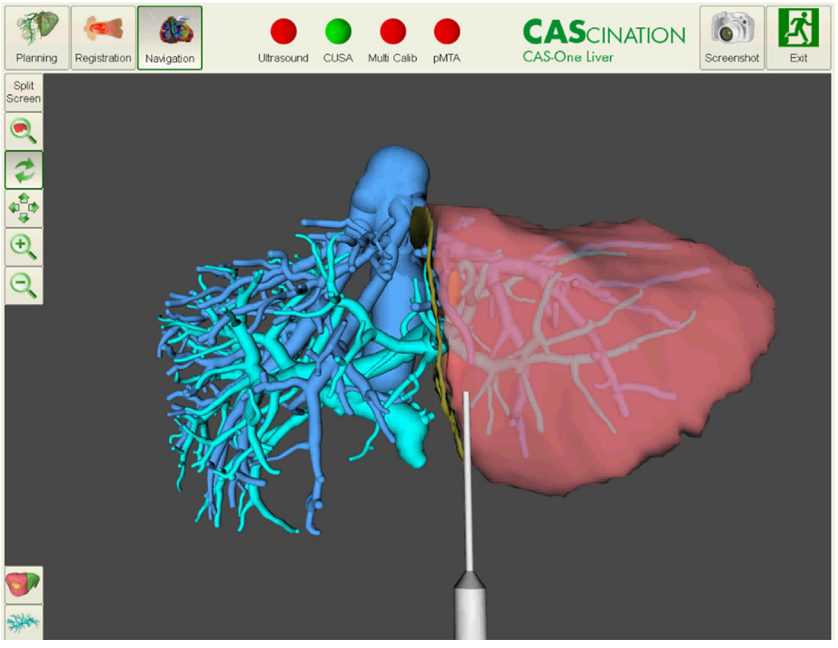

Fig. 17. CAScination utilizes MeVis virtual planning software for 3D reconstruction, liver segmentation, volumetry, and surgical simulation.

performed by the software to delineate major liver structures (eg, parenchyma, hepatic artery, portal vein, hepatic vein, and bile duct). This step is based on neighboring image vexel density of nearby structures. Third, a virtual hepatectomy is performed based on planned line of resection and sacrificed inflow. Resection volume is determined and the FLR volume is calculated based on

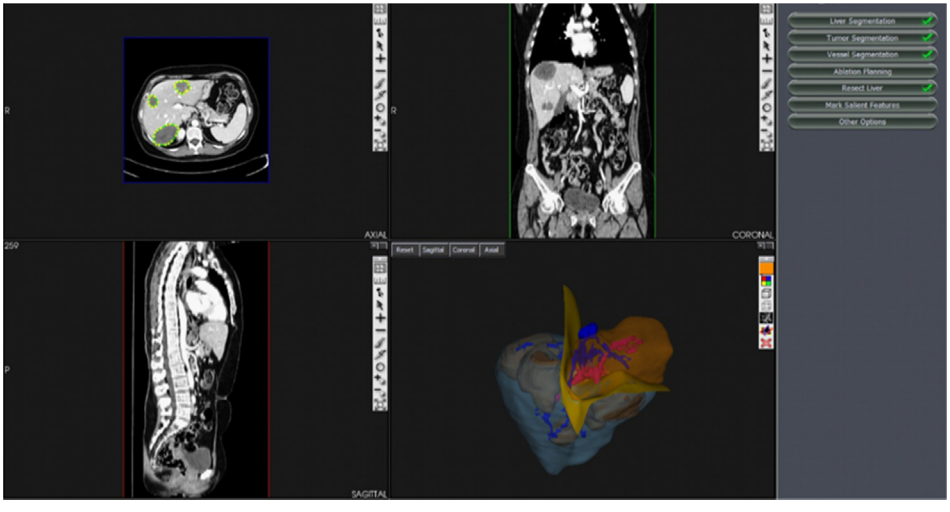

Fig. 18. Computer-assisted operating planning of virtual hepatectomy through the Pathfinder Scout system. Preoperative CT liver images are uploaded to the 3D image-processing software to perform 3D reconstruction of major liver structures. The bottom right screen image demonstrates virtual hepatectomy and the planned FLR.

remaining noncongested liver. Volumetric software allows for assessment of hepatic vein tributaries and estimated associated drainage areas. Finally, the sequence may be repeated to determine the optimal procedure. Volumetric analysis is performed based on portal perfusion, taking into account the diameter of and distance between major vessels. In this way, computer-assisted volumetry overcomes many of the shortcomings associated with hand-tracing volumetry.[60] Several studies have reported on the accuracy of computer-assisted operation planning compared to actual volumes resected.[61,62]

The 2 common scenarios where computer-assisted planning is used are complex oncologic resections and living donor liver transplantation. In cancer resections, virtual hepatectomy permits assurance of an adequate FLR based on the patient's underlying liver function[63] as well as a negative resection margin.[64] Moreover, the analysis can detail the cut surface of the liver allowing the surgeon to anticipate which vessels will be exposed. The challenge in living donor liver transplantation is ensuring adequate liver volume and function for both the donor and the recipient. Computer-assisted operation planning estimates the liver parenchyma associated with each perfusing portal pedicle as well as draining hepatic vein. A virtual hepatectomy may assist in decision making (eg, including the middle hepatic vein) and thereby confirm adequate noncongested postresection volume for both the donor and the recipient.[65-67]

Approaches to image-guided liver surgery

Registration

The first step to real-time image-guided liver surgery is matching the preoperatively obtained images to the patient's actual physical space. This process, known as registration, depends on matching correspondence between the image data sets and the patient. In contrast to other surgical fields, such as neurosurgery, orthopedics, and otolaryngology, the liver does not have a rigid frame to serve as a stereotactic reference. Furthermore, image guidance must account for mobility during respiration, differences in positioning after mobilization, and even changes in shape or contour during surgery. These factors pose significant challenges to successful and accurate registration. This section discusses various methods of registration.

Landmark, or point, based registration attempts to match corresponding anatomic points on the preoperative image data set to the patient. The challenge in landmark registration is that the liver rarely exhibits reliable points for reference. Examples that have been trialed, include the falciform ligament, vessel entrance points, and superficial tumors. Early studies that attempted to use landmark-based registration alone found identifying corresponding structures too challenging.[33,58] The preoperative placement of fiducial markers, as was done in other surgical specialties, was not feasible in liver surgery.

An alternative to landmark-based registration is surface-based correspondence. Initial acquisition of intraoperative surface data via a handheld probe was limited by surgeon skill and discipline. Laser surface scanning devices[68] can obtain a dense, regularly spaced, organ surface measurement without the noise from a handheld probe. Conoscopic holography scopes have also been trialed and may be even be more accurate.[69] Regardless of methodology, the intraoperative surface data are then registered to that of the preoperative tomogram. An iterative computer algorithm aligns the images until a successful match is found. Several challenges exist in this approach. First, liver surface scanning may result in extraneous soft tissue acquisition from surrounding structures, which eventually must be removed manually. Second, because the liver has a smooth contour, a surface based approach may permit "sliding" to an incorrect location during registration. Third, many factors during liver surgery, such as patient positioning, respiration motion, mobilization, and placement of surgical sponges, will alter the liver surface and hereby complicating or negating the registration process.

Intraoperative ultrasound offers the opportunity for real-time, accurate, and detailed information that not only may be used for diagnostic purposes but may assist with registration. The limitations of ultrasound-based registration include the large variability in image quality, owing to differences in user-dependent acquisition and programmed ultrasound settings,

and the extraction of salient information from the image data set. Once the image set is obtained, registration with the preoperative images must be completed. Intrahepatic vessels provide a convenient source for correspondence. Landmark-based registration uses vessel bifurcations as reference points. Their selection may be either automatic[70] or manual.[71] Contour-based registration takes the entire vessel into account and attempts to match the imaging sets based on vessel diameter and centerline distance.[72] Finally, intensity-based registration relies on the varying enhancement of vascular structures to create a 3D representation that can then be registered with the preoperative images. Although successfully applied in neurosurgery, challenges in accounting for deformation during surgery have not allowed application in liver surgery yet.[73]

Tracking

Although registration matches the preoperative imaging with the actual patient, it assumes that the location and orientation of the target organ remains constant. In order to account for these changes (secondary to respiration, mobilization, or resection efforts) as well as monitor the placement of surgical instruments, real-time tracking is necessary. One such method for tracking is monitoring of specially placed electromagnetic position sensors.[50] Other systems have been designed that use optical tracking of single reflective markers on the surface of the liver. Studies have demonstrated their clinical utility in the operating room and ability to account for respiratory motion and deformation.[74,75]

Alternatively, Peterhans and colleagues[73] have devised a patient-specific mesh made of biocompatible materials that can enwrap the liver, provide enhanced tracking and accommodate spatial markers and guiding holes for positioning ablation or biopsy instruments. This approach is similar to the patient-specific templates created for dental implantology[76] and is based on a virtual 3D "template" created from the patient's preoperative images. Significant limitations remain toward realizing real-time tracking. Operative navigation and true image-guided surgery will depend on the development of enhanced tracking methodologies. Because of these challenges, most registration systems use a combination of surface and point based processes.[77]

Early clinical data

Although clearly an active area of research and development, actual clinical outcome data employed image guidance technology remains scarce. Cash and colleagues[78] published the first series of patients undergoing open liver resection with the assistance of intraoperative registration and image guidance software. A total of 8 patients at Vanderbilt University and Washington University were enrolled. The Optotrak 3020 (Northern Digital, Waterloo, Ontario, Canada) optical localization system and RealScan 200C (3D Digital Corp, Sandy Hook, CT) laser range scanner were used for intraoperative registration. Surface registrations led to mean residual errors between 2 and 6 mm but typically less than 1 mm in select target areas. Finally, respiratory motion was quantified and finite element models created to account for liver deformation. Peterhans and colleagues[79] used an early CAScination system in 9 patients at the University hospital in Bern, Switzerland. Equipment set-up time was 15 minutes and registration time was approximately 1 minute. Registration errors of 10 mm were possible in most cases and the median error of the best registration per intervention was 6.3 mm. Importantly, the largest multicenter trial of image-guided liver surgery has been completed but awaits publication.[80]

Beller and colleagues[36] used a novel intraoperative 3D ultrasound with optoelectronic tracking device for central liver resections in 54 patients at the Charite hospital in Berlin, Germany. Successful navigation was possible in 96.3% of cases, with a mean histologic resection margin of 9 mm and a maximum deviation from planned surgical resection plane of 8 mm. This system has been upgraded to integrate indirect electromagnetic tracking for real-time continuous tracking of surgical instruments.[50] Kingham and colleagues[81] used tracked intraoperative ultrasound in conjunction with the Explorer system on 27 of 50 (54%) consecutive

patients at the Memorial Sloan Kettering Cancer Center. Equipment set up time was approximately 5 minutes and average registration time was less than 1 minute.

Some early clinical data has become available for laparoscopic navigation as well. Hammill and colleagues[82] described their experience with the Explorer minimally invasive liver system. A total of 27 patients underwent laparoscopic ablation procedures at Providence Portland Medical Center in Portland, Oregon, and the University of North Carolina Hospitals in Chapel Hill, North Carolina, using this experimental system. The navigation system was compared to intraoperative laparoscopic ultrasound and found to be not statistically significantly different in probe positioning. Finally, Kingham and colleagues[83] provided preliminary feasibility data on 32 patients undergoing laparoscopic liver resections using the Explorer minimally invasive liver device at the Memorial Sloan Kettering Cancer Center.

Future developments

Although tremendous advances have been made in the field of image-guided liver surgery over the past decade, additional work is still needed before image-guided systems can become routine in clinical practice. As previously described, image-guided liver surgery is limited by the nonrigid nature of the liver, as well as changes in shape and conformation of the liver after mobilization and with respiration. Ongoing research and development in nonrigid or deformable registration techniques will be necessary. The development of improved intraoperative imaging capabilities may become more available with the rise of multimodality state-of-the-art operating rooms thereby improving the accuracy of registration and tracking.[84]

The application of image guidance processes to other interventional liver techniques holds great potential. Although considered less effective than resection for most primary and metastatic liver lesions, there is still a role for radiofrequency, microwave, and cryoablation in well-selected cases.[85] Although most percutaneous ablation is performed with ultrasound or CT guidance, MRI is increasingly being used and has the advantage of improved planning, targeting and monitoring target tissue temperature and energy deposition.[86] Advancements in image-guided processes may permit more accurate placement of ablation probes, improving targeted destruction, and minimizing collateral damage.

Conclusion

Despite the inherent challenges, interest in developing image-guided systems for liver surgery is robust. Current systems, such as PTIs Explorer or CAScination's CAS-ONE, provide excellent computer-assisted operation planning with 3D volumetry in addition to basic registration and tracking. Nevertheless, clinical outcomes data on their effectiveness is still limited. Future research will focus on developing better methods of registration and tracking that account for deformation, respiratory motion, and specific anatomical constraints as well as integration with new technology in minimally invasive methods. Ultimately, the refinement of these techniques in the liver will open opportunities for the application of image guidance in other areas such as the thorax, kidney and retroperitoneum, among others.

Fluorescence in general surgery

Nicolas C. Buchs, MD, Frederic Ris, MD

Introduction

Among different fluorescent agents, indocyanine green (ICG) is probably the most used and well known in general surgery. It has been used successfully in numerous surgical procedures and has received a wide acceptance in various oncological fields, notably as a diagnostic tool for

Table 1
Characteristics of indocyanine green (ICG).

One of the few fluorescent contrast agents currently registered by the Food and Drug Administration and the European Medicines Agency for clinical applications (in addition to methylene blue and fluorescein)[88]
Well known for several decades, and was notably registered to determine cardiac output, hepatic function, and ophthalmic perfusion[88]
Sterile and water-soluble
Cheap (approximately USD $50 per patient/procedure)
Confined to the vascular compartment by binding to plasma proteins. Its plasmatic life is 3-5 minutes and its half-life 150-180 seconds
Rapidly and mainly excreted in the bile (within 10-15 minutes)[90] and does not undergo enterohepatic recirculation.[91] Physiologically, ICG appears unconjugated in bile approximately 8 minutes after injection. ICG removal from the blood depends on liver blood flow, parenchymal cellular function and biliary excretion
Very low toxicity. The risk of anaphylactic reactions is approximately 0.003% at doses exceeding 0.5 mg/kg.[92]
Absorption and emission peak of approximately 800-810 nm. This parameter is important since the near-infrared light (NIR) has a wave amplitude of 700-900 nm[87]

guiding cancer treatment.[87,88] In addition, ICG has several favorable and interesting characteristics, which contribute to its use as a good contrast agent[87,89] (Table 1).

Fluorescence-guided surgery

Several imaging systems are currently available (see the review from Gioux and colleagues[93] or Alander and colleagues[89] for a complete description), and are used all around the world. Basically, their functioning is the same, even if they differ in their technical specifications (excitation source, working distance, and field of view).[88] They all consist of a spectrally-resolved light source (filtered broadband source, light-emitting diode, or laser diode) exciting a fluorophore (ie, ICG here) within a turbid medium (ie,. blood, bile, and lymph). The light emitted from this fluorophore is then imaged onto a charge-coupled device camera, with special care taken to filter out the powerful excitation light.[93,94]

New devices are also available for laparoscopic surgery and robotic surgery. Usually, the surgeon can quickly switch between normal viewing mode (visible or white light) and NIR or fluorescence mode.[87] Superimposed images (NIR and visible light) are also possible.[95]

Main applications in general surgery

A recent review of the literature subdivided the main applications of ICG fluorescence in general surgery into 5 practical categories or fields.[87]

Visualization of vascular anatomy

Several reports mention the use of ICG for fluorescent angiography. This is not surprising as one of the first indications for ICG was the evaluation of ophthalmic perfusion.[88]

The possibilities are numerous: identification of vascular malformation, identification of segmental vascularization, evaluation of nonstandardized or nonanatomical resection that could impair the blood supply of the target organ. The interest is obvious in all surgical fields and the utility goes beyond general surgery. Vascular surgeons, urologists, ophthalmologists, and neurosurgeons have already seen the potential of this technique in a large variety of procedures.[89,96-102]

In general surgery, several authors have reported the use of this technique to identify the cystic artery during cholecystectomy.[103,104] In addition, venous flow can be also assessed with this technique.[105] The goal is to increase the safety during the dissection phase. This is especially true in the case of vascular abnormalities detected during laparoscopy. This technology could reduce the risk of conversion in these not uncommon situations.[87]

Direct injection into the portal vein was also described by a Japanese group, who showed the possibility to identify the different liver segments during hepatic resections. A clear mapping of liver segments can be obtained, even in presence of cirrhosis.[106] The system can also be used in liver transplant recipients to assess the blood flow through the vascular anastomosis.[107] Finally, as reported by Marano and collegues,[87] a real-time identification of vascular anatomy is also of great help during colorectal surgery, especially for nonstandardized resections, such as transverse or left colonic flexure resections; this could be extrapolated to all intestinal resections.

Assessment of perfusion

As a corollary of the previous indication, fluorescence can be used to assess vascular microperfusion as well. Indeed blood supply can be checked in real-time, and this can be of significant importance in order to evaluate anastomotic or flap microperfusion.[108-110] It allows an early postoperative detection of tissue necrosis in amputation stumps[111] for example.

In digestive surgery, anastomotic leakage remains one of the most dreadful complications, especially in colorectal surgery.[112,113] Among the different risk factors for anastomotic leak, the perfusion of the intestinal stump is crucial.[114] Different methods have been tried: subjective assessment (color of the bowel and pulsation in the mesentery), Doppler evaluation, oxymetry, and fluorescence of course. Several groups have reported their experience with ICG for the assessment of colorectal anastomotic perfusion. This evaluation can be done either transabdominally (in open or minimally invasive surgery) but also endscopically (transanal evaluation of the anastomosis).[115,116] When the resection was performed according to the fluorescent margin, lower rates of anastomotic leakage and complications were reported.[115] The interest is even more obvious for laparoscopic and robotic surgery where the tactile feedback is either decreased or missing. Groups using this technology have reported favorable outcomes. For example, Ris and colleagues[117] have found that a protective stoma could be avoided in case of satisfactory fluorescent perfusion. Similar findings were reported for robotic surgery, with a reduced anastomotic complications rate in the ICG group compared to standard resection (6% for ICG group vs 18% for standard group).[118] The level of transection can be also modulated as reported by Hellan and colleagues[119] who showed that fluorescence imaging provides additional data motivating to change the proximal bowel transection location in up to 40% of patients. These data are more than encouraging and should motivate further research, particularly to objectively evaluate the ICG uptake (quantitative assessment).[95] Obviously, and beyond colorectal surgery, any digestive anastomosis might be evaluated with this technology (gastric bypass and resection, esophageal surgery, and pancreatectomy) (Fig 19).

In addition, NIR fluorescence angiography can predict survival of ischemic bowel, with greater accuracy than clinical evaluation alone.[120] Not uncommonly, the surgeon is helpless in doubtful cases, especially in emergent situation. In these circumstances, ICG fluorescence can help guide the clinician's decision. A French group has reported an interesting experience of real-time navigation by fluorescence-based enhanced reality. They were able to identify the future anastomotic site in an animal model of intestinal ischemia.[121] The boundary between ischemic and vascularized zones could be detected by this technology.[122] As a word of caution, pneumoperitoneum (using CO_2 as used during laparoscopy) may increase the ICG half-life, by decreasing liver blood flow.[123] This parameter should be taken into consideration when using this technology, especially when assessing the anastomotic perfusion.

Visualization of hepatobiliary anatomy

With the introduction of minimally invasive surgery, an increased rate of biliary injury has been reported during cholecystectomy.[124] To avoid this risk, several methods have been advocated: routine use of cholangiography, use of the critical view of safety, or even a low threshold of conversion in case of any doubt. However, there is still a debate regarding the exact role of each method. In parallel, fluorescent cholangiography can be performed safely, as reported for many years by Ishizawa and colleagues,[125-127] real pioneers in this field. Their

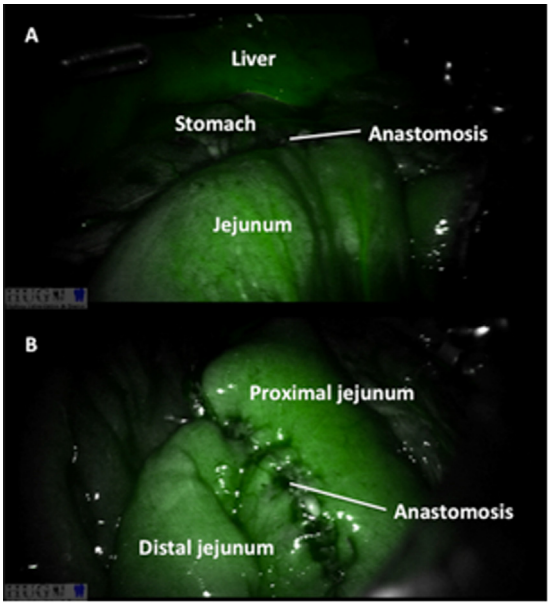

Fig. 19. Example of anastomotic perfusion using ICG during a robotic Roux-en-Y gastric bypass: (A) gastrojejunal anastomosis and (B) jejunojejunal anastomosis.

preliminary works have shown not only the feasibility and the safety of this approach, but also (and more importantly) the potential benefits to avoid biliary injury. In addition, they have shown the possibility to identify accessory biliary ducts in 8 cases (100% detection rate).[128] Because ICG is reported to be visible in the liver and the biliary tract within 20 minutes after injection,[129,130] the interest in these situations is obvious. Indeed, a high identification rate of extrahepatic biliary structures has been reported, with a detection rate of at least 93% of cystic ducts and 96% of common bile ducts (Table 2). In one of the largest robotic series, Daskalaki and colleagues[131] have confirmed these good results, with at least 1 biliary structure visualized in 99% of cases. Overall, these reports have verified the feasibility and the safety of this method (Fig 20). Moreover, ICG can really facilitate the understanding of the extrahepatic biliary anatomy, and thereby help avoiding injury[128] or misinterpretation of abnormal biliary anatomy.[128,132] Finally, ICG can be used to check the biliary anastomosis as well.[133]

In addition, there is no prolonged preparation time before start of surgery and only a negligible extension of the operation time (1-2 minutes).[103,130] This is in favor of fluorescent cholangiography, in contrast to standard cholangiography. As additional advantages over conventional cholangiography, fluorescent cholangiography is non-ionizing. Of note, biliary stones cannot be ruled out by a fluorescent cholangiography alone,[128] and thus strict selection criteria are advised.[134] Recently, Schols and colleagues[103] have reported the possibility to combine vascular and biliary fluorescence imaging during laparoscopic cholecystectomy. However, these patients required a repeated injection of ICG during the procedure in order to obtain a critical view of safety. Kaneko and colleagues[104] have reported a similar experience.

Unfortunately, in case of inflammation, the identification of extrahepatic biliary anatomy can be difficult as reported by several authors.[130,135] In addition, visceral fat can also render the identification of biliary ducts difficult. In our experience, we showed that the operative time could be shortened by the ICG technology during robotic single-site cholecystectomy. However, it was true only for patients with normal body mass index.[136] Indeed, the penetration of the NIR light is limited to 5-10 mm.[92,135] ICG can be also used for intraoperative assessment of liver anatomy during hepatic resections. A real-time road mapping of liver anatomy can be obtained. In addition, in cases of hepatocellular tumor and liver metastatic lesions, a biliary excretion

Table 2
Evaluation of extrahepatic biliary anatomy with ICG fluorescent imaging.

Study	*N*	Surgery	Dose of ICG (mg)	Time of injection	Main outcome
Schols et al[103]	30	LC	2.5*	After induction of anesthesia	Identification of CBD and CD earlier than WL (−10 minutes)
Daskalaki et al[131]	184	RC	2.5	45 min before surgery	CD, CHD, and CBD were identified in 97.8%, 94%, and 96.1%, respectively
Buchs et al[134]	12	RSSC	2.5	30-45 min before surgery	Detection of CD in 100%, CBD in 83.3% after dissection
Buchs et al[136]	23	RSSC	2.5	30-45 min before surgery	Operation faster with ICG in patients with BMI < 25
Spinoglio et al[94]	45	RSSC	2.5	30-45 min before surgery	97% of detection rate (for CD, CHD, and CBD) after dissection
Kaneko et al[104]	28	LC	0.05 mg/kg	15 min before surgery	CD Visualized in 93% and CBD in 96%
Ishizawa et al[128]	52	LC	2.5	30 min before surgery	100% Identification of CD, CBD after dissection 100% Identification of accessory hepatic ducts
Ishizawa et al[135]	7	Single-port LC	2.5	After intubation	100% Detection of confluence between CHD and CD

LC, laparoscopic cholecystectomy; RC, robotic cholecystectomy; RSSC, robotic single-site cholecystectomy; CBD, common bile duct; CD, cystic duct. CHD, common hepatic duct; WL, white light.
* Use of an iodine-free ICG (infracyanine).

disorder is found, which can contribute to better visualize the lesion (fluorescent rim in or around the tumor).[106,137-142] All of these features might help the liver surgeon identify hepatic lesions intraoperatively. Gotoh and colleagues[138] have shown that this technique helped the authors identify new nodules of hepatocellular carcinoma that were not detected by

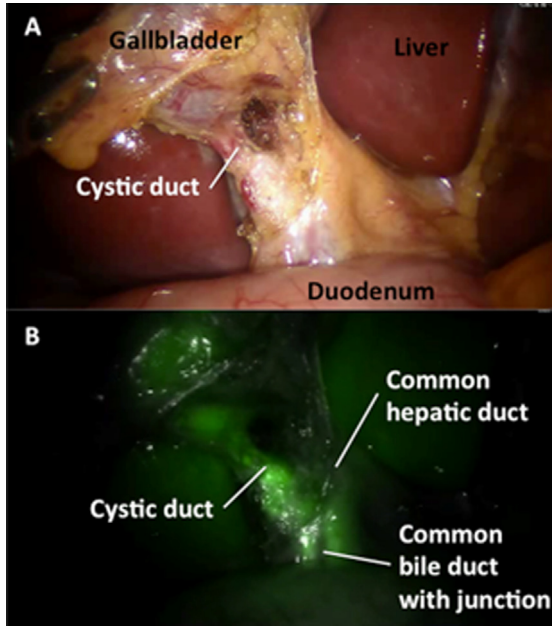

Fig. 20. Example of fluorescent cholangiography for the assessment of extrahepatic biliary anatomy. (A) Anatomy after dissection of Calot's triangle with white light. (B) Same anatomy with near-infrared light and indocyanine green.

preoperative imaging studies. The technique can also be used in minimally invasive surgery.[143,144]

The timing of injection depends on the indication, several days before surgery when identifying tumoral lesion or during surgery for road mapping.[87,88] Of note, the technique is useful only for superficial lesions. Indeed, the maximal detection depth was reported to be only 8 mm.[137]

Lymph node mapping

Since its use for breast and skin surgery,[88] the concept of sentinel lymph node biopsy (SLN) has gained general surgery among other fields.[89,145,146] Gastric surgery and colorectal surgery are the main areas where SLN detection is under evaluation in general surgery. Currently, prophylactic lymphadenectomy is considered as the standard of care for gastrointestinal cancer.[88]

In a recent review, Marano and colleagues[87] have identified 247 different patients who underwent SLN detection for gastric cancer. ICG fluorescence was endoscopically injected submucosal or subserosal, intraoperatively or before surgery. Of note, the majority of these patients were enrolled in a screening program (ie, in Japan), and had an early gastric cancer. Indeed, the clinical interest of SLN identification is more than obvious in early cancer, in order to avoid extended lymphadenectomy. Patients enrolled in these studies were mainly cT1, cT2, and cN0. Interestingly, the detection rate of the SLN ranged from 90.9%-100%.[147-153] Ichikura and colleagues[148] were able to tailor their lymphadenectomy (radical vs local) according to the result of SNL biopsy. In addition, they found that the false-negative and false-positive rates, negative predictive and positive predictive values, and accuracy for intraoperative SN biopsy were 23%, 0%, 95%, 100%, and 96%, respectively. Moreover, the simultaneous use of ICG and (99m)Tc-antimony sulfur colloid was shown to be an effective tool for SN mapping, with a sensitivity and a specificity of 100%.[150] The technique can be performed by a minimally invasive approach as well.[153,154] In one of the largest studies, Kelder and colleagues[155] have shown that the detection rate of SNL with infrared ray electronic endoscopy and ICG was better than ICG alone. A refinement of the technique is thus still possible. Finally, ongoing research needs to focus on the exact timing and the best location of the ICG injection. It seems better to inject the ICG before surgery, at least to obtain a higher detection rate of SLN and a low false-negative rate.[156]

As already mentioned, colorectal surgery is another field where SLN using ICG is gaining an increasing interest. In the same review,[87] the authors have found 157 patients involved in detection of SLN during colorectal surgery. The detection rate ranged from 88.5%-97.9%.[147,157,158] Similar findings were reported for detection of inguinal SNL in case of anal cancer.[159] Although only at its infancy, the interest of real-time SLN using ICG in colorectal surgery is obvious, even if the false-negative rate was reported to be up to 66.7% for rectal cancer.[147] Similarly to breast surgery,[160,161] a tailored approach, rather than a hyperextensive resection, is probably the future of colorectal surgery. On the other hand, SLN can be also used to decide if a more extended lateral pelvic lymph node dissection should be performed in case of low rectal cancer.[162] The same concept might be applied for complete mesocolic excision. However, today, it is difficult to justify a limited or more extended resection, based only on the SLN biopsy. Varying lymphatic drainage patterns and high rates of skip metastases have prevented the routine introduction of the SLN procedure in general clinical practice.[88]

Although ICG can be a simple and valid tool for SLN detection and lymph node mapping, the same questions and limits reported for gastric surgery exist for colorectal surgery. The time and location of injection remain a subject of debate. Contradictory studies are reported. As mentioned by Marano and colleagues,[87] a peritumoral injection before surgery can be troublesome because of inadequate or excessive diffusion of ICG around the tumor, spreading of the fluorescent dye inside the abdominal cavity. In addition, they noticed, in case of neoadjuvant radiochemotherapy for rectal cancer, that the perioperative peritumoral injection of ICG did not make visible any lymph node (possible lymphatic damage induced by radiation).

Tumor tattooing

ICG can be also used as a tattoo agent. It can be seen either with the white light or with the NIR light. Usually, the tattoo is coupled to lymph node mapping.

Several studies have reported encouraging data for colorectal surgery and pancreatic surgery.[163-165] India ink is a frequently used dye, but is associated with complications and side effects and alters the surgical field.[164] Of note, the authors recommend to perform the surgery within 8 days after endoscopic injection.[164]

Current limitations

Even if small, the risk of allergic reaction exists.[92] Strict selection criteria must be followed. An iodine-free formulation of ICG is also available, and may be used as an alternative in patients with iodine allergy.[130]

One of the main limitations of ICG use is the difficulty to analyze the quantity of the signal (objective evaluation). Most of the studies presented herein focused on the quality of ICG (subjective assessment: yes or no or maybe) but not really on the quantity of the signal (objective assessment). Schols and colleagues[103] have proposed such an analysis where the fluorescence images were examined by determining target-to-background ratio (TBR). TBR was defined as the mean fluorescence intensity (FI) of 2-point regions of interest (ROIs) in the target (ie, structures of the biliary tract in this situation) minus the mean FI of 2 background ROIs in the liver hilum, divided by the mean FI of the 2 background ROIs in the liver hilum. Although relatively complicated to assess during the operation, they were able to show a clear delineation (high TBR) of the structures of interest. New software that could assess in vivo the quantity of ICG is needed, especially for analyzing the real-time perfusion, as recently reported for evaluating the duodenal perfusion in pancreas transplantation.[166]

In addition, with the current technology, the tissue penetration of the fluorescence emitted by ICG is only 5-10 mm. It is difficult to identify tumor located deep in the liver,[137,142] to detect a SNL in massive adipose tissue[155] or to visualize anatomical structures in obese patients or inflamed tissues.[136]

Future developments in fluorescence

More specific agents are required. Indeed, false positive lesions have been reported, notably in hepatibiliary surgery field.[137,138] Recently, Schols and colleagues[167] have reported interesting results using a new NIR dye (CW800-CA) showing the same characteristics as ICG. They found that fluorescent cholangiography of the cystic duct could be obtained earlier (− 10 minutes) with the new dye in comparison to ICG. Similar findings were reported by other groups.[168]

In a recent study on the swine, a group from Harvard has shown the possibility to inject 2 different contrast agents: methylene blue for biliary anatomy and zwitterionic NIR fluorophore ZW800-1 for vascular anatomy. They were able to show that this combination provided simultaneous, real-time, and high-resolution identification of bile ducts and hepatic arteries during biliary tract surgery.[169] This is of special interest for future development of new and more specific contrast dyes. For colorectal metastasis, another group has reported encouraging results using an integrin targeting NIR fluorescence probe.[170]

In the colorectal field, ureteral injury during laparoscopic resection is a rare but serious complication with a reported incidence rate of 0.28%.[171] The early detection and prevention of ureteral injury is clinically relevant and important in order to avoid this complication.[172] New developments in this field include the use of fluorescent stents,[95] use of specific fluorescent dye,[172] and use of augmented reality.[112,173] The use of augmented reality and fluorescence to assess the intestinal perfusion is also gaining an increased interest.[121,122] Further clinical work is required to confirm the encouraging results obtained in animal-model. Finally, all this knowledge needs to be shared in dedicated societies. The emergence of associations with a special focus on the development of ICG guided surgery is mandatory (www.figss.net).

The creation of an international registry is also essential to promote the progress of this technology.

Technical challenges and future perspectives

Stéphane Nicolau, Luc Soler, Jacques Marescaux, MD

Displaying information to surgeons in laparoscopic surgery

The general aim of computer-assisted surgery is to provide specific information that will help surgeons during a specific task. As already mentioned, this information is usually displayed on a screen or directly in the surgeon's field of view using augmented reality wearable glasses. In this section, we describe the different ways by which information can be shown using the paradigm of augmented virtuality and augmented reality.

Augmented virtuality

The concept of augmented virtuality was first introduced by Milgram and Kishino.[174] In our surgical context, it consists of displaying the instrument positions (endoscopic camera and any kind of tool) and the patient position in a virtual scene. The instruments are usually visualized using an avatar with a virtual shape close or not to their real one (Fig 21) and the patient as either a 3-dimensional (3D) multiplanar image, or a volume rendering or a group of 3D models extracted from a preoperative image[34,175-177] (Fig 21). Sometimes a combination of these options can be provided depending on the surgeon needs. Obviously, the patient shape cannot be approximated from a general model as the patient anatomy varies too much from one patient to another. The instrument positions in this virtual scene are updated in real-time according to their motion in the real world. These positions are commonly provided by a commercial optical or electromagnetic tracking system, which follows the instrument motions using optical or electromagnetic (EM) markers attached to them. The virtual scene, containing virtual objects only, is thus augmented by information from the real world and this approach can therefore be named augmented virtuality. Although the patient model shape or position could also be updated in real-time, there is, to the best of our knowledge, no augmented virtuality system in laparoscopic surgery that proposes such real-time virtual organ model update.

Augmented reality

Data projection on patient

The method that seems the quickest to bring augmented reality (AR) in the operating room is the projection of information directly on the patient (Fig 22). The idea is to show directly on the patient skin or organ surface, which is visible to all staff in the operating room, the position of organs and structures of interest.[178-182] We already explained in a previous article that this approach has to be carefully handled as it can mislead the surgeon.[183] Indeed, the projected information depth will be well interpreted by the brain only if the user is located almost at the same position as the projector, otherwise a naive interpretation will provide erroneous information. Usually, the user is aware of this phenomenon and will take it into account by mentally modifying his or her interpretation, yet it is user dependent.

Practically, the projection-based AR on the patient is well adapted to show the planned trocar positions, the incisions, and structures that are located just under the skin, like spine, ribs, specific muscles, and vessels.

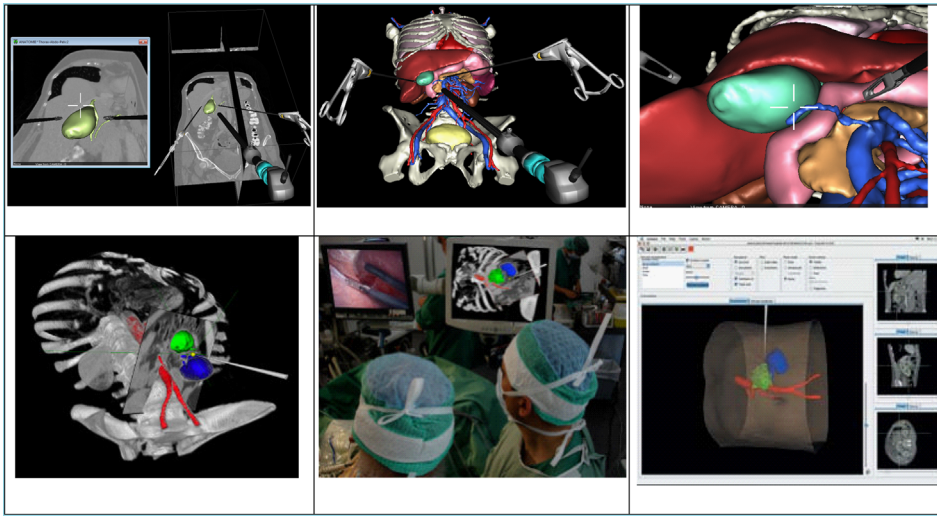

Fig. 21. Illustration of augmented virtuality based navigation systems. Top row shows a 3D patient model using CT scan data only (left) or 3D model (middle) associated to the instrument positions, which are updated in real-time thanks to a commercial tracking system.[176,177] The left image displays a simulation of the endoscopic view, updated as well from the camera position. The bottom left image shows a volume rendering view of a patient, combined with 3D models of 3 structures of interest and a crop of a CT scan slice in a specific orientation, orthogonal to the instrument. The bottom middle image shows how this image is displayed in the operating room, and the right image shows a different visualization mode, focusing on the virtual instrument position with respect to the patient 3D model only.[4] (Source: courtesy of Thomas Lango, SINTEF, Norway.)

Data superimposition on tablet personal computer

The growth of tablet personal computer (PC) in everyday life has modified the operating room conditions since most surgeons own a tablet PC and handle it with a great expertise. The tablet PC can be taken anywhere and its interactions are performed directly with fingers and are highly intuitive. Since the development of the application visible patient (http://www.visiblepatient.eu; available on AppleStore and GoogleStore), our own experience in our abdominal surgery team is clear and shows that surgeons are not reluctant at all to visualize and handle 3D patient models at medical staff meetings[184] or even in the operating room (using a sterile bag encapsulating a tablet PC).

Within this context, the emergence of the tablet PC naturally gave birth to software applications that display the patient 3D model on the video of the tablet PC back camera[185] (Fig 23). Some of them are dedicated to instrument placement allowing to display the organ

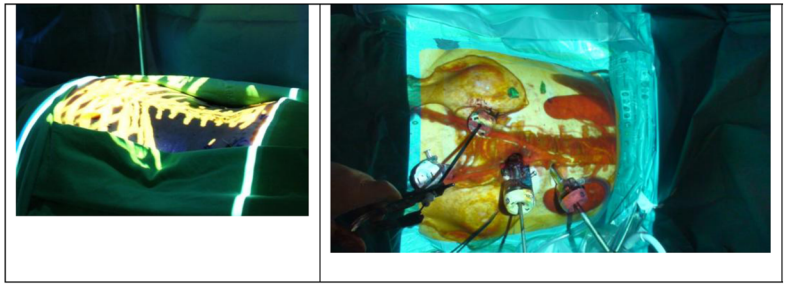

Fig. 22. Illustration of patient model directly projected on patient skin or organ surface. *Left*: spine and ribs are projected on the patient back to guide orthopedic surgeon. (Source: courtesy of Kai-Che Liu and Pei-Yuan Lee, Asian Institute of TeleSurgery, Chang Bing Show Chwan Memorial Hospital.)[8] *Right*: Organs are projected on the patient abdomen to optimize the trocar insertion.[9] (Source: courtesy of Dr. Francesco Volonté, Service de Chirurgie Viscérale et de Transplantation, Hôpitaux Universitaires de Genève.)[182]

Fig. 23. *Left image*: tablet PC overlays preoperative patient 3D model using landmarks, which are automatically tracked in the video using image processing. (Source: courtesy of Prof. H.P. Meinzer, DKFZ, Heidelberg.) *Right image*[185]: surgeons manually register the preoperative 3D model of the liver, its vessels and its lesions using anatomical landmarks directly visible in open surgery. (Source: courtesy of Dr. Schenk, Fraunhofer Institute for Medical Image Computing MEVIS©.)

models superimposed on the patient view, the superimposition being updated in real-time thanks to dedicated markers. Surgeons can thus visually evaluate the best positions for all instruments and incisions.[186,187] Other applications are dedicated to open hepatic surgery (http://www.ipadguides.net/mitk-pille-mobile-medicaql-augmented-reality-app-for-the-apple-ipad.html) to show the liver vessels, segments, and tumors before any resection. The registration in this example is performed manually thanks to visible anatomical landmarks. All these applications are still prototypes of research labs, not commercialized, and do not certify the overlay accuracy.

Data superimposition in see-through glasses

Although it is technically more complex to design such a solution for the operating room compared to the previous one, the idea of augmenting the direct view of surgeons using wearable AR-glasses or a semitransparent screen was first proposed in the early 1990s. It is indeed possible to overlay medical data in the direct view of the surgeon using either projection on semitransparent mirrors[188-194] or integral videography located between the surgeon's eyes and the patient[195-198] (Fig 24). One can easily imagine the benefits of these kinds of tools for open surgery procedures. Surgeons could overlay when necessary supplementary information under an organ surface.

In the context of endoscopic surgery, these approaches are interesting to display planning information related to outer patient parts. Some research work even proposed to use AR-glasses in order to display a virtual scene mimicking the real one at the location of the surgery so that surgeons keep their eyes focused on the patient's abdomen.[199] However, the virtual scene currently cannot be sufficiently realistic to allow such a paradigm. Moreover, it is not clear whether this approach really provides any benefit for the surgeon or not.

Fig. 24. Illustration of some systems providing guidance information directly in the practitioner field of view, using see-through technology. *Left*: the integral videography system for needle puncture assistance is positioned above the patient.[28] *Right*: example of integral videography showing the jaw position using a see-through approach. (Source: courtesy of Prof. Hongen Liao, Department of Biomedical Engineering, School of Medicine, Tsinghua University.)

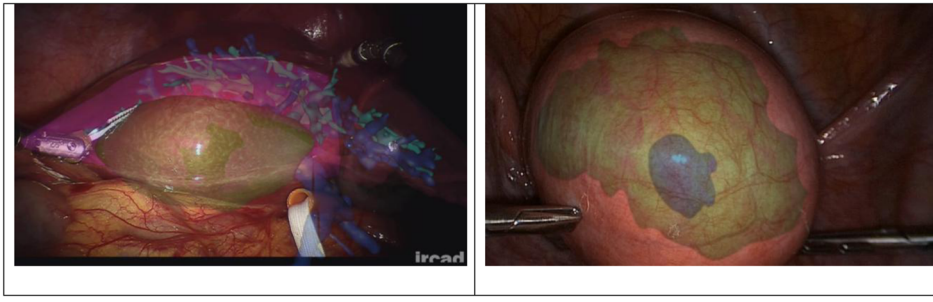

Fig. 25. Illustration of augmented reality overlay in endoscopic surgery. *Left*: a liver tumor (in green), its surrounding vessels (dark and light blue) and the resection plane (in pink) are displayed.[14] *Right*: 2 myomas inside a uterus are superimposed in a gynecological surgery context.[35] (Source: courtesy of Prof. Adrien Bartoli, ALCOV, Université de Clermont-Ferrand.)

Data superimposition with the laparoscopic camera

As surgeons perform the surgery watching a screen, it seems perfectly appropriate to superimpose critical information on the object that attracts most of their attention. Practically, most of the work related to AR in endoscopic surgery overlays supplementary information directly on the surgical screen (Fig 25). Usually, software displays in the screen either a preoperative 3D model (deformable or not)[53,173,183,184,200-205] or real-time ultrasound (US) images acquired by a laparoscopic transducer during surgery.[173,206-208] Obviously, the superimposed information is displayed only when necessary and requested by the surgeon.

Superimposition of the information in the correct position

The common word usually employed by scientists to describe the proper alignment of the augmented information in the real surgical view is registration (and sometimes fusion). This step generally consists in computing the rotation and translation (or pose) of the 3D preoperative model of the patient so that it corresponds to the real position of the patient structures. This computation can only be performed using acquired information in the operating room and many approaches have been proposed in the last decade, all the more since recent progress now allows to take deformation into account.

Registration based on different data types

The oldest but easiest solution allowing to register a preoperative 3D patient model is to stick external markers on the patient skin, these fiducials being visible in the preoperative data and acquired in the operating room thanks to a tracking system. For this approach to provide an acceptable accuracy, the marker acquisition in the operating room must be performed before patient insufflation. If not, the 3D marker configuration is too different from the one extracted in the preoperative image. Note that these markers can be anatomical (iliac crest, umbilicus, nipple, and ribs). This means that this approach is generally relevant to provide an AR view of the whole patient abdomen, and thus mainly useful for instrument positioning. In laparoscopic renal surgery, Nakamoto and colleagues[205] proposed to use implantable EM wireless landmarks, which are attached to the kidney, tracked in real-time and manually identified on the preoperative model of the kidney for registration. With the endoscopic camera being also localized by the EM tracking system, it is then easy to superimpose the 3D kidney model in the endoscopic image.

The second approach to obtain relevant data for registration is to use an intraoperative imaging device during the surgery. Shekhar and colleagues[209] use interventional computed tomography (CT), its frame position being calibrated with respect to an optical tracking system. With the endoscopic camera also being tracked by the tracking system, this allows then a direct superimposition of the CT data rendered with volume rendering in the endoscopic image.

A similar solution has been proposed by Feuerstein and colleagues,[210] Bernhardt and colleagues,[211] and Oktay and colleagues[212] but using a rotational C-arm, with the assumption that a new 3D volume image is acquired each time that it is necessary for the surgeon (due to additional deformation for instance). Baumhauer and colleagues[213] intraoperatively attach several small needles in the organ of interest and acquire, using a 3D rotational C-arm, a volume image of the organ, which is registered to the preoperative model using the surface only. Then the small needles are tracked in real-time in the endoscopic images, allowing for registration of the preoperative model. Konishi and colleagues[53] and Feuerstein and colleagues[214] proposed to use a US laparoscopic probe tracked by an optical tracking system for picking the intra-operative position of liver vessels to be registered with a preoperative model or directly superimposed in the endoscopic image. In cardiac surgery, CARTO suite software from Biosense Webster proposed to acquire the heart surface using a catheter tracked by an EM system, then registered with iterative closest point algorithm[215,216] to the preoperative heart model.[217-219]

As surgeons generally prefer to avoid any additional equipment, which may modify or disturb the standard surgical workflow, many research works have focused on techniques allowing to recover organ surface from the live endoscopic image only.[220] Mountney and colleagues,[224] Stoyanov and colleagues,[223] Lee and colleagues,[222] and Röhl and colleagues[221] typically used a stereoscopic endoscope to reconstruct organ surface using stereovision technique (needing a calibration step before the surgery begins). Mountney and colleagues,[227] Hu and colleagues,[225] Mahmoud and colleagues,[228] and Garcia and colleagues[226] proposed a solution to estimate the organ surface from the camera motion with simultaneous localization and mapping or structure from motion technique, the main idea being that parallax motion is sufficient to understand the scene shape. Other teams also use image information only, shading,[229,230] and shape assumption[231,232] (using conformal model), to estimate the organ surface with satisfactory results.

Other approaches to acquire organ surface in real-time require improvement of endoscopic devices to add a structured light projector or time-of-flight miniaturized equipment.[233] Such devices may allow surface acquisition from combined processing of video image and supplementary data provided by the miniaturized equipment.

Finally, the last well-known approach consists in the tracking of anatomical landmarks, manually or automatically selected or recognized in the endoscopic image, tracked in real-time thanks to their significant texture,[194,234-236] which are matched to their corresponding points in the preoperative model. In this case, the difficult step is the detection of anatomical landmarks in the endoscopic image, which is currently fully interactive. It is indeed very difficult to automatically and robustly recognize on images of different patients the same anatomical structures. This means that a user must select in the live endoscopic image the relevant anatomical landmarks along the surgery.

Registration model

Once information describing the localization of a part of the structure of interest is available, it is then possible to register the 3D preoperative model on the information that has been acquired. The main question at this step is to choose the registration type: rigid or nonrigid.

Rigid model

This is the model used by the CAS-ONE Liver from CAScination for open surgery, described earlier. The system registers a rigid preoperative liver model using anatomical landmarks (vessel bifurcations) acquired using an ultrasound probe, tracked by an optical tracking system. An algorithm then estimates a rotation and a translation (also called pose) to apply to the preoperative 3D model so that the anatomical landmarks extracted from the model are superimposed as close as possible to the corresponding landmarks in the video image for instance. If the data used for registration is surface, a rigid registration of surface also consists of determining the rotation and the translation that best fit the surface from the preoperative model with the surface (often incomplete) acquired during surgery. We recall here that rotation and translation can each be parameterized by 3 values. Although rigid

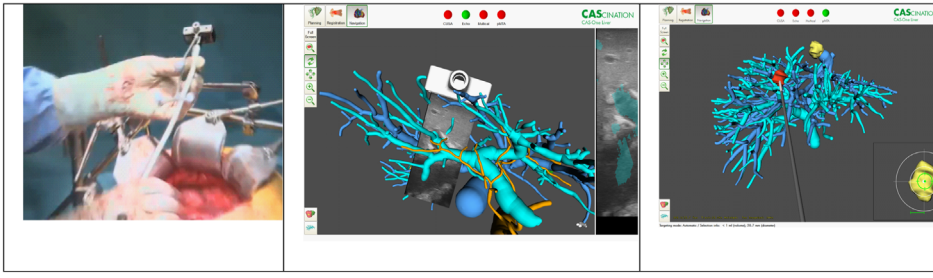

Fig. 26. CAS-ONE Liver from CAScination© is a navigation system that allows to rigidly register a preoperative model of liver vessels on a set of sparse 2D ultrasound images. Left: the ultrasound probe is localized by an optical tracking system. After ultrasound images acquisitions and vessel extraction from 2D ultrasound image, a rigid registration is performed allowing to display the live 2D ultrasound image position (middle[85]) or an instrument (right) with the preoperative model of the liver vessel. (Source: courtesy of Dr. Matthias Peterhans, CAScination©.)

assumption is known to be wrong, they assume that it is locally acceptable for smaller liver parts, typically 1 or 2 connected segments. Information is then provided using an augmented virtuality paradigm; the position of an ultrasound image is overlaid in a common frame with the 3D preoperative model (Fig 26).

In the context of endoscopic surgery, interactive augmented reality, where expert assistance is necessary to manually register the liver preoperative model, has proven to be useful and sufficiently accurate for liver, pancreatic, and adrenal gland surgery.[179-181,204] Other research work demonstrated similar results for the kidney, since it undergoes little deformation during a mini-invasive surgery, thus allowing the rigid model to remain a good approximation.[202,203]

Deformable model

Nonrigid registration has been considered by many researchers for a long time and led to several deformable models. Describing most of them in detail does not seem to us very relevant since they can involve mathematically complex background. We will only provide a simplified interpretation of the most famous approaches. The affine deformable model basically allows a deformation of the preoperative 3D model in each direction of space without volume constraint. This deformation needs the identification of at least 4 landmarks in both the 3D preoperative model and the live data. This model cannot take important flexion into account, yet only elongation or compression.[231,236]

The free-form B-spline and thin-plate spline based models are much more general than the affine model and can allow very complex deformation as long as numerous corresponding landmarks roughly along a grid have been identified in the preoperative 3D model and acquired in real-time during surgery.[237-239] Practically, few landmarks are usually acquired and the grid size is big and its resolution is low, which leads to a deformation model that is nonlinear, compared to linear affine model, but still limited if the number and location of landmarks are not sufficient and well spread.

More recent work involves using preoperative 3D model based on tetrahedron meshes, which allows the inclusion of biomechanical properties (typically Young's modulus and Poisson's ratio).[200,240-242] The main advantage of this approach is that it ensures a realistic deformation is applied as long as appropriate parameters have been set into the model, which will be discussed further. Real-time solution can easily be provided if the number of tetrahedra is reasonable but hardly fulfil real-time constraints in a more complex scenario where several organs collide themselves.

Discussion: Challenges and open problems

Despite the amount of research work in the field of AR, there are extremely few commercial solutions to guide surgeons during laparoscopic surgery. Moreover, these solutions do not certify

the guidance information provided by the software; the responsibility is thus borne by the medical expert. In this section, we discuss the reasons explaining this fact and propose some alternatives or approaches that may allow to provide faster image guidance tools to surgeons.

The main difficulty, which has prevented many research works from being set up in an OP room, is the current impossibility to predict the accuracy of the AR superimposition on the laparoscopic image. In the surgical context, there is currently no tool to compute the system accuracy after a deformation has been applied to a preoperative model, using landmarks, the detection error of which is statistically known. It is also obvious that a rigid registration cannot properly mimic a deformable organ like the liver,[243-245] and it is also currently not possible to accurately estimate the subsequent superimposition error. One solution is to develop a biomechanical model of the organ of interest, the mechanical properties of which are sufficiently close to patient ones, and a method allowing to realistically estimate the tissue deformation from a set of anatomical landmarks, the position of which is tracked in real-time. This solution raises the issue of determining the mechanical property of an organ before or during surgery, keeping in mind that the liver, for instance, contains 3 vessel networks that necessarily locally modify its mechanical properties and heat functions. There are some ultrasound transducers, that propose an estimation of the biomechanical properties of the scanned tissue (Airexplorer from Supersonic Imagine). One can also find some work on reverse estimation of tissue properties from an analysis of the motion feedback after interaction with a tool.[246] However, these methods are still limited to a local estimation, far from a complete scanning of an entire organ.

Assuming now that such accurate prediction method would exist, one would still face the validation issue. Indeed, to perform a validation of the superimposition accuracy, it is necessary to know the ground truth, (eg, the exact contour position of the structure of interest in the endoscopic image). Currently the most rigorous validation protocol relies on image acquisitions of the structure of interest with an ultrasound probe, for which the position in 3D is tracked by an EM tracking system. From a set of 2D ultrasound images that are localized in space, it is possible to determine after image analysis the position of the structure of interest in the EM tracking system frame. The endoscopic camera being also tracked by the EM system, it is thus theoretically possible to compute the location of the structure of interest in the endoscopic image. However, this information is not accurate due to the numerous error sources that are statistically added: EM tracking system error on the ultrasound probe ($\sim$1 mm) and on the endoscopic camera ($\sim$1 mm), calibration of the endoscopic camera optical center ($\sim$1 mm), calibration of the ultrasound probe image location ($\sim$1 mm), and ultrasound image analysis error ($\sim$1 mm).

Recently a new approach has been proposed avoiding most of these calibration steps. It consists of acquiring a 3D volume image that contains both the patient and the endoscope,[196] the endoscopic camera position being computed from an analysis of the 3D volume image. Authors claim an accuracy of a few millimeters (corresponding to a few pixels), however their work involves a 3D rotational C-arm that does not provide images with good quality due to artefact and low dose imaging. Moreover, it relies on the assumption that the manufacturing of the endoscope is close to a perfect cylinder and that the optical axis is perfectly parallel to the endoscope shaft direction, which cannot be guaranteed. However, the principle seems relevant and may provide sufficient accuracy with a CT-scan. This work must still be confirmed by further experiments on both phantom and in vivo data. If a rigorous analysis of all parameters can allow to link them to a pixel accuracy function in the endoscopic image, then it will be feasible to obtain a certification for a system.

Despite the difficulty to compute and ensure guiding system accuracy for laparoscopic surgery, we believe that such systems should be developed and proposed now on the market. Indeed, it is more and more accepted that even manually registered information bring relevant guidance information. This has been seen on commercial products for interventional radiology and for open surgery, which indicate after the registration process that the guidance information may not be totally reliable and that the guidance responsibility is borne by the surgeon or the radiologist. Although one could criticize that companies are providing a useless system, this point of view is erroneous. The MyLab70 system from Esaote Medical (as well as Acuson S3000

from Siemens and LOGIQ E9 from GE Healthcare) allows to register automatically and manually a preoperative CT scan on a live ultrasound volume image, this volume being a set of 2D ultrasound images acquired whereas the ultrasound probe is being localized by a EM tracking system. The registration accuracy is not certified and a message is thus displayed to the user indicating that the CT scan image superimposition on the live ultrasound is just a rough guidance information and that the user must rely on the live US image only. In other words, the user has the right to believe or not believe the registration obtained (from the consistency of anatomical landmarks superimposition). Practically, the user often manually adapts the first registration provided by the automatic algorithm, mostly because of breathing deformation. Therefore, it seems relevant to let the user decide whether their own registration is proper or not.

In open surgery, the same paradigm has been proposed by CAScination[79,247] and Pathfinder.[248,249] For instance, CAS-ONE Liver software from CAScination allows registration of a preoperative CT or magnetic resonance imaging scan to a live acquisition of a set of 2D ultrasound images (the ultrasound probe being tracked by an optical tracking system). The registration model is rigid and thus may undergo important errors due to liver deformations between the preoperative and intraoperative states. However, even if the information is not perfectly accurate, the user is able to visually assess the misregistration error from the virtual scene (for instance the discrepancy between the predicted vessel positions and the true ones provided by the ultrasound probe) and obtain sufficient information to guide the operation. Let's imagine that a tumor in the liver is close to a vein bifurcation, and that the user could clearly see on the virtual view that the bifurcation is misregistered by 1 cm in the cranio-caudal direction. From this visual assessment, the user can then predict and mentally correct the misregistration and thus obtain insight about the true tumor position.

These existing commercial systems are therefore extremely relevant to improve the medical outcome. However, it seems important to stress another crucial benefit of the development of such systems, for which accuracy is not certified. Indeed, for a research study to be carried out in a clinical environment on a patient, many administrative steps must be fulfilled, particularly if the research work involves an equipment without medical CE or Food and Drug Administration approval. The fostering of commercial guiding systems, which are certified for the operating room but without accuracy certification, seems therefore dramatically important to speed up research work. For instance, thanks to the MyLab70, Acuson S3000 or LOGIQ E9 system, it becomes extremely easy to acquire on a patient live 2D ultrasound images with their space localization, whereas many calibration algorithms have to be developed and tested, and documents have to be written and submitted to the institutional review board (IRB) if researchers have to attach by themselves an optical marker to the US probe. Research and medical studies can go on much faster thanks to these commercial and medically certified products.

These discussions lead to the following conclusion: it seems relevant to develop guiding systems for endoscopic surgery, their registration process being performed manually, keeping in mind that the manual interactions may be reduced thanks to research progress on intra-operative data acquisition and analysis. Regarding the latter, there are 2 paradox trends: hybrid surgical rooms including an intraoperative scanning device are more and more popular and at the same time most literature analyses report that it is better to avoid modifying the standard clinical workflow so that a product can be quickly clinically accepted. We believe both approaches are pertinent and not necessarily incompatible. On the one hand, the research performed with costly equipment in the operating room to obtain intraoperative guidance information is important to quantitatively assess to what extent intraoperative guiding systems can help practitioners (eg, intervention duration, safety, confidence). If the benefits are real but the cost unacceptable (eg, money, time preparation, sterility constraints, and freedom movement in the operating room), other research is then valuable to decrease the remaining drawbacks. On the other hand, it is extremely appropriate to try to develop guiding systems using the current available data in the operating room only (typically analysis of the endoscopic video to recover the tissue motion or biological properties). Indeed, in this case, there is no need to modify the equipment. However, it may be necessary to lengthen some exploration phases to

get optimal images, and thus to modify the procedure itself, for further processes. It is then necessary to check that such changes are easily tolerated by practitioners.

Regarding the visualization approach to guide endoscopic surgery, it is worth highlighting that the augmented virtuality paradigm has not been extensively used in laparoscopic surgery. This seems normal for several reasons: difficult hand eye coordination as the virtual scene point of view is not necessarily the one of practitioner; and swapping from the real endoscopic view to the screen displaying the virtual scene may be confusing. On the contrary, in the case of needle insertion for neurosurgery or interventional radiology, since the patient is not open and as there is no possible view at the needle tip, watching the patient is irrelevant and the medical expert is used to watch either the control fluoroscopy or the ultrasound image to manipulate the needle. In this context, the point of view may be awkward and difficult to interpret (particularly in case of 2D projections provided by a C-arm) and augmented virtuality is thus relevant.[99] For these reasons, the choice of superimposing a 3D model in an endoscopic image is coherent, even if the method to render the information is still debated and under analysis.[250] One may argue that augmented virtuality could be used as previously proposed for natural orifice translumenal endoscopic surgery (NOTES),[251,252] to show in a virtual scene the position of the flexible endoscope with respect to the surrounding organs. Such guidance interface is very interesting for NOTES due to the common disorientation issues during exploration. However, such an approach is more questionable in laparoscopic surgery since the endoscope located in the abdominal cavity is rigidly manipulated by the surgeon and orientation is thus well controlled and understood.

Conclusions

Computer-guiding systems for endoscopic surgery are entering the operating room, even if certification of their accuracy is still an issue. It is interesting to mention that a Swiss company (Lausanne) called 2C3D SA had been launched in 2000 to provide AR assistance using interactive registration in digestive endoscopic surgery. However, despite its relevant help the product did not encounter a great success, certainly because practitioners were still not used to using 3D models for their surgery and also because they were waiting for automatic registration tools, which do not modify their usual clinical workflow. Fifteen years later, there is still no product proposing automatic and accuracy certified registration, but practitioners accept using a PC tablet in the operating room and perform interactive registration.

Mentalities have changed, communication in medical specialties has never been so intensive, and there are now more and more free or costless applications of interest, available on smartphone or PC tablet that can be tested in the operating room. This seems to have modified the relationship between surgeons and technology and fostered the development of new guidance systems for surgical applications. Moreover, there are more and more computer scientists with strong experience of the operating room who are able to understand the clinical constraints, and there are more surgeons with experience of computer technologies. This phenomenon obviously increases the likelihood of developing new systems that are really relevant and helpful for the patients, the surgeons and society.

References

1. Bucholz RD. Introduction to Journal of Image Guided Surgery. *J Image Guid Surg*. 1995;1(1):1–3.
2. Blomstedt P, Olivecrona M, Sailer A, Hariz MI. Dittmar and the history of stereotaxy; or rats, rabbits, and references. *Neurosurgery*. 2007;60(1):198–201. [discussion 2].
3. al-Rodhan NR, Kelly PJ. Pioneers of stereotactic neurosurgery. *Stereotact Funct Neurosurg*. 1992;58(1-4):60–66.
4. Rahman M, Murad GJ, Mocco J. Early history of the stereotactic apparatus in neurosurgery. *Neurosurg Focus*. 2009;27(3):E12.
5. Horsley V, Clarke RH. The structure and functions of the cerebellum examined by a new method. *Brain, 31*. Oxford, UK: Oxford University Press; 1908; p 45–124.
6. Spiegel EA, Wycis HT, Marks M, Lee AJ. Stereotaxic Apparatus for Operations on the Human Brain. *Science*. 1947;106 (2754):349–350.
7. Galloway Jr RL. The process and development of image-guided procedures. *Annu Rev Biomed Eng*. 2001;3:83–108.

8. Danish SF, Baltuch GH. History of deep brain stimulation. In: Baltuch GH, Stern MB, editors. *Deep Brain Stimulation for Parkinson's Disease*. Boca Raton, FL: CRC Press; 2007:1–15.
9. Bergström M, Greitz T. Stereotaxic computed tomography. *Am J Roentgenol*. 1976;127:167–170.
10. Brown RA. A stereotactic head frame for use with CT body scanners. *Invest Radiol*. 1979;14(4):300–304.
11. Jacques S, Shelden CH, McCann GD. Freshwater DB, Rand R. Computerized three-dimensional stereotaxic removal of small central nervous system lesions in patients. *J Neurosurg*. 1980;53(6):816–820.
12. Kelly PJ, Alker Jr. GJ, Goerss S. Computer-assisted stereotactic microsurgery for the treatment of intracranial neoplasms. *Neurosurgery*. 1982;10(3):324–331.
13. Roberts DW, Strohbehn JW, Hatch JF, Murray W, Kettenberger H. A frameless stereotaxic integration of computerized tomographic imaging and the operating microscope. *J Neurosurg*. 1986;65(4):545–549.
14. Kosugi Y, Watanabe E, Goto J, et al. An articulated neurosurgical navigation system using MRI and CT images. *IEEE Trans Biomed Eng*. 1988;35(2):147–152.
15. Watanabe E, Watanabe T, Manaka S, Mayanagi Y, Takakura K. Three-dimensional digitizer (neuronavigator): new equipment for computed tomography-guided stereotaxic surgery. *Surg Neurol*. 1987;27(6):543–547.
16. Bucholz RD. *System for indicating the position of a surgical probe within a head on an image of the head*. 1995.
17. Bucholz R, McDurmont L. The history, current status, and future of the stealthstation treatment guidance system. *Textbook of Stereotactic and Functional Neurosurgery*.Berlin, Heidelberg: Springer; 2009; p 543–565.
18. Heilbrun MP, McDonald P, Wiker C, Koehler S, Peters W. Stereotactic localization and guidance using a machine vision technique. *Stereotactic and functional neurosurgery*.Karger Publishers; 1992; p 94–98.
19. Heilbrun MP, McDonald P, Wiker JC, Koehler S, Peters W. *Apparatus and method for photogrammetric surgical localization*. 1995.
20. Allen GS. *Fiducial implant and system of such implants*. 1995.
21. Schreiner S, Lewis JT, Allen GS, Galloway RLJ. Technique for the three-dimensional localization of implanted fiducial markers. *Med Imaging*. 1995:148–160.
22. Henderson JM, Smith KR, Bucholz RD. An accurate and ergonomic method of registration for image-guided neurosurgery. *Comput Med Imaging Graph*. 1994;18(4):273–277.
23. Bucholz RD, Smith KR, Henderson JM, McDurmont LL, Schulze DW, eds Intraoperative localization using a three-dimensional optical digitizer. *OE/LASE'93: Optics, Electro-Optics, & Laser Applications in Science& Engineering*. 1993.
24. Smith KR, Frank KJ, Bucholz RD. The NeuroStation–a highly accurate, minimally invasive solution to frameless stereotactic neurosurgery. *Comput Med Imaging Graph*. 1994;18(4):247–256.
25. Peters T, Cleary K. Image-Guided Interventions: Technology and Applications. In: Peters T, Cleary K, editors. *Image-Guided Interventions: Technology and Applications*. New York: Springer; 2008:28–31.
26. Leksell L. Stereotactic radiosurgery. *J Neurol Neurosurg Psychiatry*. 1983;46(9):797–803.
27. Adler JR. *Apparatus for and method of performing sterotaxic surgery*. 1993.
28. Jethwa PR, Barrese JC, Gowda A, Shetty A, Danish SF. Magnetic resonance thermometry-guided laser-induced thermal therapy for intracranial neoplasms: initial experience. *Neurosurgery*. 2012;71(1 suppl operative): 133–144. [44-45].
29. Willie JT, Laxpati NG, Drane DL, et al. Real-time magnetic resonance-guided stereotactic laser amygdalohippocampotomy for mesial temporal lobe epilepsy. *Neurosurgery*. 2014;74(6):569–584. [discussion 84-5].
30. Herline AJ, Herring JL, Stefansic JD, Chapman WC, Galloway Jr RL, Dawant BM. Surface registration for use in interactive, image-guided liver surgery. *Comput Aided Surg*. 2000;5(1):11–17.
31. Helm P, Teichman R, Hartmann S, Simon D. Spinal Navigation and Imaging: History, Trends and Future. *IEEE Trans Med Imaging*. 2015.
32. Strong EB. Image-guided functional endoscopic sinus surgery. *Curr Opin Otolaryngol Head Neck Surg*. 2000;8:3–6.
33. Herline AJ, Stefansic JD, Debelak JP, et al. Image-guided surgery: preliminary feasibility studies of frameless stereotactic liver surgery. *Arch Surg*. 1999;134(6):644–649. [discussion 9-50].
34. Marvik R, Lango T, Tangen GA, et al. Laparoscopic navigation pointer for three-dimensional image-guided surgery. *Surg Endosc*. 2004;18(8):1242–1248.
35. Herline A, Stefansic JD, Debelak J, Galloway RL, Chapman WC. Technical advances toward interactive image-guided laparoscopic surgery. *Surg Endosc*. 2000;14(7):675–679.
36. Beller S, Hunerbein M, Eulenstein S, Lange T, Schlag PM. Feasibility of navigated resection of liver tumors using multiplanar visualization of intraoperative 3-dimensional ultrasound data. *Ann Surg*. 2007;246(2):288–294.
37. Sindram D, McKillop IH, Martinie JB, Iannitti DA. Novel 3-D laparoscopic magnetic ultrasound image guidance for lesion targeting. *HPB (Oxford)*. 2010;12(10):709–716.
38. Adhikari S, Blaivas M, Lyon M, Shiver S. Transfer of real-time ultrasound video of FAST examinations from a simulated disaster scene via a mobile phone. *Prehosp Disaster Med*. 2014;29(3):290–293 http://dx.doi.org/10.1017/S1049023X14000375. [Epub 2014 Apr 16].
39. Kern SJ, Smith RS, Fry WR, Helmer SD, Reed JA, Chang FC. Sonographic examination of abdominal trauma by senior surgical residents. *Am Surg*. 1997;63(8):669–674.
40. Frezza EE, Solis RL, Silich RJ, Spence RK, Martin M. Competency-based instruction to improve the surgical resident technique and accuracy of the trauma ultrasound. *Am Surg*. 1999;65(9):884–888.
41. Berber E, Siperstein A. Local recurrence after laparoscopic radiofrequency ablation of liver tumors: an analysis of 1032 tumors. *Ann Surg Oncol*. 2008;15(10):2757–2764 http://dx.doi.org/10.1245/s10434-008-0043-7. [Epub 2008 Jul 11].
42. Tanis E, Nordlinger B, Mauer M, et al. Local recurrence rates after radiofrequency ablation or resection of colorectal liver metastases. Analysis of the European Organisation for Research and Treatment of Cancer 40004 and 40983. *Eur J Cancer*. 2014;50(5):912–919 http://dx.doi.org/10.1016/j.ejca.2013.12.008. [Epub 4 Jan 7].
43. Swan RZ, Sindram D, Martinie JB, Iannitti DA. Operative microwave ablation for hepatocellular carcinoma: complications, recurrence, and long-term outcomes. *J Gastrointest Surg*. 2013;17(4):719–729.

44. Kennedy TJ, Cassera MA, Khajanchee YS, Diwan TS, Hammill CW, Hansen PD. Laparoscopic radiofrequency ablation for the management of colorectal liver metastases: 10-year experience. *J Surg Oncol*. 2013;107(4):324–328.
45. Brass P, Hellmich M, Kolodziej L, Schick G, Smith AF. Ultrasound guidance versus anatomical landmarks for internal jugular vein catheterization. *Cochrane Database Syst Rev*. 2015;1:CD006962 http://dx.doi.org/10.1002/14651858.CD006962.pub2.
46. Sobolev M, Slovut DP, Lee Chang A, Shiloh AL, Eisen LA. Ultrasound-Guided Catheterization of the Femoral Artery: A Systematic Review and Meta-Analysis of Randomized Controlled Trials. *J Invasive Cardiol*. 2015;27(7):318–323.
47. Harms J, Feussner H, Baumgartner M, Schneider A, Donhauser M, Wessels G. Three-dimensional navigated laparoscopic ultrasonography: first experiences with a new minimally invasive diagnostic device. *Surg Endosc*. 2001;15(12):1459–1462.
48. Sjolie E, Lango T, Ystgaard B, Tangen GA, Nagelhus Hernes TA, Marvik R. 3D ultrasound-based navigation for radiofrequency thermal ablation in the treatment of liver malignancies. *Surg Endosc*. 2003;17(6):933–938.
49. Bao P, Sinha TK, Chen CC, Warmath JR, Galloway RL, Herline AJ. A prototype ultrasound-guided laparoscopic radiofrequency ablation system. *Surg Endosc*. 2007;21(1):74–79.
50. Beller S, Eulenstein S, Lange T, Hunerbein M, Schlag PM. Upgrade of an optical navigation system with a permanent electromagnetic position control: a first step towards "navigated control" for liver surgery. *J Hepatobiliary Pancreat Surg*. 2009;16(2):165–170.
51. Franz AM, Marz K, Hummel J, et al. Electromagnetic tracking for US-guided interventions: standardized assessment of a new compact field generator. *Int J Comput Assist Radiol Surg*. 2012;7(6):813–818.
52. Kleemann M, Hildebrand P, Birth M, Bruch HP. Laparoscopic ultrasound navigation in liver surgery: technical aspects and accuracy. *Surg Endosc*. 2006;20(5):726–729.
53. Konishi KNMK, Tanoue Y, Kawanaka K, et al. A real-time navigation system for laparoscopic surgery based on three-dimensional ultrasound using magneto-optic hybrid tracking configuration. *Int J CARS*. 2007;2:1–10.
54. Lango T, Vijayan S, Rethy A, et al. Navigated laparoscopic ultrasound in abdominal soft tissue surgery: technological overview and perspectives. *Int J Comput Assist Radiol Surg*. 2012;7(4):585–599.
55. Sindram D, Swan RZ, Lau KN, McKillop IH, Iannitti DA, Martinie JB. Real-time three-dimensional guided ultrasound targeting system for microwave ablation of liver tumours: a human pilot study. *HPB (Oxford)*. 2011;13(3):185–191.
56. Sindram D, Simo KA, Swan RZ, et al. Laparoscopic microwave ablation of human liver tumours using a novel three-dimensional magnetic guidance system. *HPB (Oxford)*. 2015;17(1):87–93.
57. Jarnagin WR, Gonen M, Fong Y, et al. Improvement in perioperative outcome after hepatic resection: analysis of 1,803 consecutive cases over the past decade. *Ann Surg*. 2002;236(4):397–406. [discussion -7].
58. Chapman WC, Galloway RL. Image-Guided Liver Surgery. Intraoperative Imaging and Image-Guided Therapy. In: Jolesz FA, editor. *Image-Guided Liver Surgery. Intraoperative Imaging and Image-Guided Therapy*. New York, NY: Springer Science; 2014.
59. Mise Y, Tani K, Aoki T, et al. Virtual liver resection: computer-assisted operation planning using a three-dimensional liver representation. *J Hepato-Biliary-Pancreat Sci*. 2013;20:157–164.
60. Suzuki K, Epstein ML, Kohlbrenner R, et al. Quantitative radiology: automated CT liver volumetry compared with interactive volumetry and manual volumetry. *Am J Roentgenol*. 2011;197(4):W706–W712.
61. van der Vorst JR, van Dam RM, van Stiphout RS, et al. Virtual liver resection and volumetric analysis of the future liver remnant using open source image processing software. *World J Surg*. 2010;34(10):2426–2433.
62. Dello SAWG, Stoot JHMB, van Stiphout RSA, et al. Prospective volumetric assessment of the liver on a personal computer by nonradiologists prior to partial hepatectomy. *World J Surg*. 2011;35(2):386–392.
63. Simpson AL, Geller DA, Hemming AW, et al. Liver planning software accurately predicts postoperative liver volume and measures early regeneration. *J Am Coll Surg*. 2014;219:199–207.
64. Yamanaka J, Saito S, Fujimoto J. Impact of preoperative planning using virtual segmental volumetry on liver resection for hepatocellular carcinoma. *World J Surg*. 2007;31:1249–1255.
65. Yamanaka J, Saito S, Iimuro Y, et al. The impact of 3-D virtual hepatectomy simulation in living-donor liver transplantation. *J Hepatobiliary Pancreat Surg*. 2006;13:363–369.
66. Radtke A, Nadalin S, Sotiropoulos GC, et al. Parenchyma transection in adult live donor liver transplantation: the virtual dilemma of "where to cut". Experience based on virtual 3-dimensional computed tomography imaging reconstructions. *Hepatogastroenterology*. 2006;53:811–815.
67. Radtke A, Sotiropoulos GC, Sgourakis G, et al. "Anatomical" versus "territorial" belonging of the middle hepatic vein: virtual imaging and clinical repercussions. *J Surg Res*. 2011;166:146–155.
68. Cash DM, Sinha TK, Chapman WC, et al. Incorporation of a laser range scanner into image-guided liver surgery: surface acquisition, registration, and tracking. *Med Phys*. 2003;30:1671–1682.
69. Simpson AL, Burgner J, Glisson CL, et al. Comparison study of intraoperative surface acquisition methods for surgical navigation. *IEEE Trans Biomed Eng*. 2013;60:1090–1099.
70. Nowatschin S, Markert M, Weber S, Lueth TC, eds. A system for analyzing intraoperative B-Mode ultrasound scans of the liver. 29th Annual International Conference of the IEEE Engineering in Medicine and Biology Society, EMBS 2007; August 2007.
71. Lange T, Papenberg N, Heldmann S, et al. 3D ultrasound-CT registration of the liver using combined landmark-intensity information. *Int J Comput Assist Radiol Surg*. 2009;4:79–88.
72. Ojdanic D, Zidowitz S, Peitgen H. Vessel-based intraoperative rigid registration for navigated liver surgery: first experiences. In: Graser, Ristic-Durrant, editors. *Methods and Applications in Automation: 30th-31st Colloquium of Automation*. Salzhausen/Leer, Germany: Shaker Verlag GmbH; 2010.
73. Peterhans M, Candinas D, Weber S. Soft tissue navigation and liver surgery support. In: Jolesz FA, editor. *Intraoperative Imaging and Image-Guided Therapy*. New York, NY: Springer Science; 2014.
74. Markert M, Koschany A, Lueth T. Tracking of the liver for navigation in open surgery. *Int J Comput Assist Radiol Surg*. 2010;5:229–235.

75. Oliveira-Santos T, Peterhans M, Hofmann S, Weber S. Passive single marker tracking for organ motion and deformation detection in open liver surgery. In: Taylor RH, Yang G-Z, editors. *Information Processing in Computer-Assisted Interventions. Lecture Notes in Computer Science*. Berlin, Heidelberg: Springer; 2011:156–167.
76. Nickenig H-J, Eitner S, Rothamel D, Wichmann M, Zöller JE. Possibilities and limitations of implant placement by virtual planning data and surgical guide templates. *Int J Comput Dent*. 2012;15:9–21.
77. Clements LW, Chapman WC, Dawant BM, Galloway RL, Miga MI. Robust surface registration using salient anatomical features for image-guided liver surgery: algorithm and validation. *Med Phys*. 2008;35:2528–2540.
78. Cash DM, Miga MI, Glasgow SC, et al. Concepts and preliminary data toward the realization of image-guided liver surgery. *J Gastrointest Surg*. 2007;11:844–859.
79. Peterhans M, vom Berg A, Dagon B, et al. A navigation system for open liver surgery: design, workflow and first clinical applications. *Int J Med Robot*. 2011;7:7–16.
80. *ClinicalTrials.gov*. Evaluation of Image-Guided Liver Surgical System for Resection of Liver Cancer. Available from: http://clinicaltrials.gov/ct2/show/NCT00782886.
81. Kingham TP, Scherer MA, Neese BW, Clements LW, Stefansic JD, Jarnagin WR. Image-guided liver surgery: intraoperative projection of computed tomography images utilizing tracked ultrasound. *HPB (Oxford)*. 2012;14(9):594–603.
82. Hammill CW, Clements LW, Stefansic JD, Wolf RF, Hansen PD, Gerber DA. Evaluation of a minimally invasive image-guided surgery system for hepatic ablation procedures. *Surg Innov*. 2014;21(4):419–426.
83. Kingham TP, Jayaraman S, Clements LW, Scherer MA, Stefansic JD, Jarnagin WR. Evolution of image-guided liver surgery: transition from open to laparoscopic procedures. *J Gastrointest Surg*. 2013;17:1274–1282.
84. Jolesz F. Introduction. Intraoperative Imaging and Image-Guided Therapy. In: Jolesz FA, editor. *Introduction. Intraoperative Imaging and Image-Guided Therapy*. New York, NY: Springer Science; 2014.
85. Gravante G, Overton J, Sorge R, et al. Radiofrequency ablation versus resection for liver tumours: an evidence-based approach to retrospective comparative studies. *J Gastrointest Surg*. 2011;15:378–387.
86. Terraz S, Salomir R, Becker C. MR-guided radiofrequency ablation of liver tumours. In: Jolesz FA, editor. *Intraoperative Imaging and Image-Guided Therapy*. New York, NY: Springer Science; 2014.
87. Marano A, Priora F, Lenti LM, Ravazzoni F, Quarati R, Spinoglio G. Application of fluorescence in robotic general surgery: review of the literature and state of the art. *World J Surg*. 2013;37(12):2800–2811.
88. Schaafsma BE, Mieog JS, Hutteman M, et al. The clinical use of indocyanine green as a near-infrared fluorescent contrast agent for image-guided oncologic surgery. *J Surg Oncol*. 2011;104(3):323–332.
89. Alander JT, Kaartinen I, Laakso A, et al. A review of indocyanine green fluorescent imaging in surgery. *Int J Biomed Imaging*. 2012;2012:940585.
90. Shimizu S, Kamiike W, Hatanaka N, et al. New method for measuring ICG Rmax with a clearance meter. *World J Surg*. 1995;19(1):113–118. discussion 8.
91. Faybik P, Hetz H. Plasma disappearance rate of indocyanine green in liver dysfunction. *Transplant Proc*. 2006;38(3):801–802.
92. Speich R, Saesseli B, Hoffmann U, Neftel KA, Reichen J. Anaphylactoid reactions after indocyanine-green administration. *Ann Intern Med*. 1988;109(4):345–346.
93. Gioux S, Choi HS, Frangioni JV. Image-guided surgery using invisible near-infrared light: fundamentals of clinical translation. *Mol Imaging*. 2010;9(5):237–255.
94. Spinoglio G, Priora F, Bianchi PP, et al. Real-time near-infrared (NIR) fluorescent cholangiography in single-site robotic cholecystectomy (SSRC): a single-institutional prospective study. *Surg Endosc*. 2013;27(6):2156–2162.
95. Cahill RA, Ris F, Mortensen NJ. Near-infrared laparoscopy for real-time intra-operative arterial and lymphatic perfusion imaging. *Colorectal Dis*. 2011;13(suppl 7):12–17.
96. Perry D, Bharara M, Armstrong DG, Mills J. Intraoperative fluorescence vascular angiography: during tibial bypass. *J Diabetes Sci Technol*. 2012;6(1):204–208.
97. Borofsky MS, Gill IS, Hemal AK, et al. Near-infrared fluorescence imaging to facilitate super-selective arterial clamping during zero-ischaemia robotic partial nephrectomy. *BJU Int*. 2013;111(4):604–610.
98. Krane LS, Manny TB, Hemal AK. Is near infrared fluorescence imaging using indocyanine green dye useful in robotic partial nephrectomy: a prospective comparative study of 94 patients. *Urology*. 2012;80(1):110–116.
99. Litvack ZN, Zada G, Laws Jr ER. Indocyanine green fluorescence endoscopy for visual differentiation of pituitary tumor from surrounding structures. *J Neurosurg*. 2012;116(5):935–941.
100. Yamamoto S, Kim P, Kurokawa R, Itoki K, Kawamoto S. Selective intraarterial injection of ICG for fluorescence angiography as a guide to extirpate perimedullary arteriovenous fistulas. *Acta Neurochir*. 2012;154(3):457–463.
101. Hosono M, Sasaki Y, Sakaguchi M, Suehiro S. Intraoperative fluorescence imaging during surgery for coronary artery fistula. *Interact Cardiovasc Thorac Surg*. 2010;10(3):476–477.
102. Tanaka E, Chen FY, Flaumenhaft R, Graham GJ, Laurence RG, Frangioni JV. Real-time assessment of cardiac perfusion, coronary angiography, and acute intravascular thrombi using dual-channel near-infrared fluorescence imaging. *J Thorac Cardiovasc Surg*. 2009;138(1):133–140.
103. Schols RM, Bouvy ND, van Dam RM, Masclee AA, Dejong CH, Stassen LP. Combined vascular and biliary fluorescence imaging in laparoscopic cholecystectomy. *Surg Endosc*. 2013;27(12):4511–4517.
104. Kaneko J, Ishizawa T, Masuda K, et al. Indocyanine green reinjection technique for use in fluorescent angiography concomitant with cholangiography during laparoscopic cholecystectomy. *Surg Laparosc Endosc Percutan Tech*. 2012;22(4):341–344.
105. Kai K, Satoh S, Watanabe T, Endo Y. Evaluation of cholecystic venous flow using indocyanine green fluorescence angiography. *J Hepato-Biliary-Pancreat Sci*. 2010;17(2):147–151.
106. Aoki T, Murakami M, Yasuda D, et al. Intraoperative fluorescent imaging using indocyanine green for liver mapping and cholangiography. *J Hepato-Biliary-Pancreat Sci*. 2010;17(5):590–594.

107. Mitsuhashi N, Kimura F, Shimizu H, et al. Usefulness of intraoperative fluorescence imaging to evaluate local anatomy in hepatobiliary surgery. *J Hepatobiliary Pancreat Surg*. 2008;15(5):508–514.
108. Nguyen JT, Ashitate Y, Buchanan IA, et al. Bone flap perfusion assessment using near-infrared fluorescence imaging. *J Surg Res*. 2012;178(2):e43–e50.
109. Nguyen JT, Ashitate Y, Buchanan IA, et al. Face transplant perfusion assessment using near-infrared fluorescence imaging. *J Surg Res*. 2012;177(2):e83–e88.
110. Lee BT, Matsui A, Hutteman M, et al. Intraoperative near-infrared fluorescence imaging in perforator flap reconstruction: current research and early clinical experience. *J Reconstr Microsurg*. 2010;26(1):59–65.
111. Zimmermann A, Roenneberg C, Wendorff H, Holzbach T, Giunta RE, Eckstein HH. Early postoperative detection of tissue necrosis in amputation stumps with indocyanine green fluorescence angiography. *Vasc Endovasc Surg*. 2010;44(4):269–273.
112. Buchs NC, Ris F, Jung M, Morel P. New trends in robotic colorectal surgery. *Adv Robot Autom*. 2014;3(1):e117.
113. Buchs NC, Gervaz P, Secic M, Bucher P, Mugnier-Konrad B, Morel P. Incidence, consequences, and risk factors for anastomotic dehiscence after colorectal surgery: a prospective monocentric study. *Int J Colorectal Dis*. 2008;23(3):265–270.
114. Vignali A, Gianotti L, Braga M, Radaelli G, Malvezzi L, Di Carlo V. Altered microperfusion at the rectal stump is predictive for rectal anastomotic leak. *Dis Colon Rectum*. 2000;43(1):76–82.
115. Kudszus S, Roesel C, Schachtrupp A, Hoer JJ. Intraoperative laser fluorescence angiography in colorectal surgery: a noninvasive analysis to reduce the rate of anastomotic leakage. *Langenbecks Arch Surg*. 2010;395(8):1025–1030.
116. Sherwinter DA, Gallagher J, Donkar T. Intra-operative transanal near infrared imaging of colorectal anastomotic perfusion: a feasibility study. *Colorectal Dis*. 2013;15(1):91–96.
117. Ris F, Hompes R, Cunningham C, et al. Near-infrared (NIR) perfusion angiography in minimally invasive colorectal surgery. *Surg Endosc*. 2014;28(7):2221–2226.
118. Jafari MD, Lee KH, Halabi WJ, et al. The use of indocyanine green fluorescence to assess anastomotic perfusion during robotic assisted laparoscopic rectal surgery. *Surg Endosc*. 2013;27(8):3003–3008.
119. Hellan M, Spinoglio G, Pigazzi A, Lagares-Garcia JA. The influence of fluorescence imaging on the location of bowel transection during robotic left-sided colorectal surgery. *Surg Endosc*. 2014;28(5):1695–1702.
120. Matsui A, Winer JH, Laurence RG, Frangioni JV. Predicting the survival of experimental ischaemic small bowel using intraoperative near-infrared fluorescence angiography. *Br J Surg*. 2011;98(12):1725–1734.
121. Diana M, Dallemagne B, Chung H, et al. Probe-based confocal laser endomicroscopy and fluorescence-based enhanced reality for real-time assessment of intestinal microcirculation in a porcine model of sigmoid ischemia. *Surg Endosc*. 2014.
122. Diana M, Noll E, Diemunsch P, et al. Enhanced-reality video fluorescence: a real-time assessment of intestinal viability. *Ann Surg*. 2014;259(4):700–707.
123. Tunon MJ, Gonzalez P, Jorquera F, Llorente A, Gonzalo-Orden M, Gonzalez-Gallego J. Liver blood flow changes during laparoscopic surgery in pigs. A study of hepatic indocyanine green removal. *Surg Endosc*. 1999;13(7):668–672.
124. Adamsen S, Hansen OH, Funch-Jensen P, Schulze S, Stage JG, Wara P. Bile duct injury during laparoscopic cholecystectomy: a prospective nationwide series. *J Am Coll Surg*. 1997;184(6):571–578.
125. Ishizawa T, Tamura S, Masuda K, et al. Intraoperative fluorescent cholangiography using indocyanine green: a biliary road map for safe surgery. *J Am Coll Surg*. 2009;208(1):e1–e4.
126. Kawaguchi Y, Ishizawa T, Masuda K, et al. Hepatobiliary surgery guided by a novel fluorescent imaging technique for visualizing hepatic arteries, bile ducts, and liver cancers on color images. *J Am Coll Surg*. 2011;212(6):e33–e39.
127. Ishizawa T, Bandai Y, Hasegawa K, Kokudo N. Fluorescent cholangiography during laparoscopic cholecystectomy: indocyanine green or new fluorescent agents? *World J Surg*. 2010;34(10):2505–2506.
128. Ishizawa T, Bandai Y, Ijichi M, Kaneko J, Hasegawa K, Kokudo N. Fluorescent cholangiography illuminating the biliary tree during laparoscopic cholecystectomy. *Br J Surg*. 2010;97(9):1369–1377.
129. Schols RM, Bouvy ND, van Dam RM, Stassen LP. Advanced intraoperative imaging methods for laparoscopic anatomy navigation: an overview. *Surg Endosc*. 2013;27(6):1851–1859.
130. Schols RM, Bouvy ND, Masclee AA, van Dam RM, Dejong CH, Stassen LP. Fluorescence cholangiography during laparoscopic cholecystectomy: a feasibility study on early biliary tract delineation. *Surg Endosc*. 2013;27(5):1530–1536.
131. Daskalaki D, Fernandes E, Wang X, et al. Indocyanine green (ICG) fluorescent cholangiography during robotic cholecystectomy: results of 184 consecutive cases in a single institution. *Surg Innov*. 2014.
132. Calatayud D, Milone L, Elli EF, Giulianotti PC. ICG-fluorescence identification of a small aberrant biliary canaliculus during robotic cholecystectomy. *Liver Int*. 2012;32(4):602.
133. Hutteman M, van der Vorst JR, Mieog JS, et al. Near-infrared fluorescence imaging in patients undergoing pancreaticoduodenectomy. *Eur Surg Res*. 2011;47(2):90–97.
134. Buchs NC, Hagen ME, Pugin F, et al. Intra-operative fluorescent cholangiography using indocyanin green during robotic single site cholecystectomy. *Int J Med Robot*. 2012;8(4):436–440.
135. Ishizawa T, Kaneko J, Inoue Y, et al. Application of fluorescent cholangiography to single-incision laparoscopic cholecystectomy. *Surg Endosc*. 2011;25(8):2631–2636.
136. Buchs NC, Pugin F, Azagury DE, et al. Real-time near-infrared fluorescent cholangiography could shorten operative time during robotic single-site cholecystectomy. *Surg Endosc*. 2013;27(10):3897–3901.
137. Ishizawa T, Fukushima N, Shibahara J, et al. Real-time identification of liver cancers by using indocyanine green fluorescent imaging. *Cancer*. 2009;115(11):2491–2504.
138. Gotoh K, Yamada T, Ishikawa O, et al. A novel image-guided surgery of hepatocellular carcinoma by indocyanine green fluorescence imaging navigation. *J Surg Oncol*. 2009;100(1):75–79.

139. Ishizuka M, Kubota K, Kita J, Shimoda M, Kato M, Sawada T. Intraoperative observation using a fluorescence imaging instrument during hepatic resection for liver metastasis from colorectal cancer. *Hepatogastroenterology*. 2012;59(113):90–92.
140. Yokoyama N, Otani T, Hashidate H, et al. Real-time detection of hepatic micrometastases from pancreatic cancer by intraoperative fluorescence imaging: preliminary results of a prospective study. *Cancer*. 2012;118(11):2813–2819.
141. Uchiyama K, Ueno M, Ozawa S, et al. Combined intraoperative use of contrast-enhanced ultrasonography imaging using a sonazoid and fluorescence navigation system with indocyanine green during anatomical hepatectomy. *Langenbecks Arch Surg*. 2011;396(7):1101–1107.
142. Kokudo N, Ishizawa T. Clinical application of fluorescence imaging of liver cancer using indocyanine green. *Liver Cancer*. 2012;1(1):15–21.
143. Ishizawa T, Zuker NB, Kokudo N, Gayet B. Positive and negative staining of hepatic segments by use of fluorescent imaging techniques during laparoscopic hepatectomy. *Arch Surg*. 2012;147(4):393–394.
144. Kudo H, Ishizawa T, Tani K, et al. Visualization of subcapsular hepatic malignancy by indocyanine-green fluorescence imaging during laparoscopic hepatectomy. *Surg Endosc*. 2014;28(8):2504–2508.
145. Holloway RW, Bravo RA, Rakowski JA, et al. Detection of sentinel lymph nodes in patients with endometrial cancer undergoing robotic-assisted staging: a comparison of colorimetric and fluorescence imaging. *Gynecol Oncol*. 2012;126(1):25–29.
146. Rossi EC, Ivanova A, Boggess JF. Robotically assisted fluorescence-guided lymph node mapping with ICG for gynecologic malignancies: a feasibility study. *Gynecol Oncol*. 2012;124(1):78–82.
147. Kusano M, Tajima Y, Yamazaki K, Kato M, Watanabe M, Miwa M. Sentinel node mapping guided by indocyanine green fluorescence imaging: a new method for sentinel node navigation surgery in gastrointestinal cancer. *Dig Surg*. 2008;25(2):103–108.
148. Ichikura T, Chochi K, Sugasawa H, et al. Individualized surgery for early gastric cancer guided by sentinel node biopsy. *Surgery*. 2006;139(4):501–507.
149. Lee JH, Ryu KW, Kook MC, et al. Feasibility of laparoscopic sentinel basin dissection for limited resection in early gastric cancer. *J Surg Oncol*. 2008;98(5):331–335.
150. Park, do J, Kim HH, et al. Simultaneous indocyanine green and (99m)Tc-antimony sulfur colloid-guided laparoscopic sentinel basin dissection for gastric cancer. *Ann Surg Oncol*. 2011;18(1):160–165.
151. Miyashiro I, Miyoshi N, Hiratsuka M, et al. Detection of sentinel node in gastric cancer surgery by indocyanine green fluorescence imaging: comparison with infrared imaging. *Ann Surg Oncol*. 2008;15(6):1640–1643.
152. Park DJ, Lee HJ, Lee HS, et al. Sentinel node biopsy for cT1 and cT2a gastric cancer. *Eur J Surg Oncol*. 2006;32(1):48–54.
153. Tajima Y, Murakami M, Yamazaki K, et al. Sentinel node mapping guided by indocyanine green fluorescence imaging during laparoscopic surgery in gastric cancer. *Ann Surg Oncol*. 2010;17(7):1787–1793.
154. Miyashiro I, Kishi K, Yano M, et al. Laparoscopic detection of sentinel node in gastric cancer surgery by indocyanine green fluorescence imaging. *Surg Endosc*. 2011;25(5):1672–1676.
155. Kelder W, Nimura H, Takahashi N, Mitsumori N, van Dam GM, Yanaga K. Sentinel node mapping with indocyanine green (ICG) and infrared ray detection in early gastric cancer: an accurate method that enables a limited lymphadenectomy. *Eur J Surg Oncol*. 2010;36(6):552–558.
156. Tajima Y, Yamazaki K, Masuda Y, et al. Sentinel node mapping guided by indocyanine green fluorescence imaging in gastric cancer. *Ann Surg*. 2009;249(1):58–62.
157. Cahill RA, Anderson M, Wang LM, Lindsey I, Cunningham C, Mortensen NJ. Near-infrared (NIR) laparoscopy for intraoperative lymphatic road-mapping and sentinel node identification during definitive surgical resection of early-stage colorectal neoplasia. *Surg Endosc*. 2012;26(1):197–204.
158. Hirche C, Mohr Z, Kneif S, et al. Ultrastaging of colon cancer by sentinel node biopsy using fluorescence navigation with indocyanine green. *Int J Colorectal Dis*. 2012;27(3):319–324.
159. Hirche C, Dresel S, Krempien R, Hunerbein M. Sentinel node biopsy by indocyanine green retention fluorescence detection for inguinal lymph node staging of anal cancer: preliminary experience. *Ann Surg Oncol*. 2010;17(9):2357–2362.
160. Kitai T, Inomoto T, Miwa M, Shikayama T. Fluorescence navigation with indocyanine green for detecting sentinel lymph nodes in breast cancer. *Breast Cancer*. 2005;12(3):211–215.
161. Tagaya N, Yamazaki R, Nakagawa A, et al. Intraoperative identification of sentinel lymph nodes by near-infrared fluorescence imaging in patients with breast cancer. *Am J Surg*. 2008;195(6):850–853.
162. Noura S, Ohue M, Seki Y, et al. Feasibility of a lateral region sentinel node biopsy of lower rectal cancer guided by indocyanine green using a near-infrared camera system. *Ann Surg Oncol*. 2010;17(1):144–151.
163. Watanabe M, Tsunoda A, Narita K, Kusano M, Miwa M. Colonic tattooing using fluorescence imaging with light-emitting diode-activated indocyanine green: a feasibility study. *Surg Today*. 2009;39(3):214–218.
164. Miyoshi N, Ohue M, Noura S, et al. Surgical usefulness of indocyanine green as an alternative to India ink for endoscopic marking. *Surg Endosc*. 2009;23(2):347–351.
165. Ashida R, Yamao K, Okubo K, et al. Indocyanine green is an ideal dye for endoscopic ultrasound-guided fine-needle tattooing of pancreatic tumors. *Endoscopy*. 2006;38(2):190–192.
166. Garcia-Roca R, Walczak D, Tzvetanov I, Khan A, Oberholzer J. The application of indocyanine green to evaluate duodenal perfusion in pancreas transplantation. *Am J Transplant*. 2014;14(1):226–228.
167. Schols RM, Lodewick TM, Bouvy ND, et al. Near-infrared fluorescence laparoscopy of the cystic duct and artery in pigs: performance of a preclinical dye. *J Laparoendosc Adv Surg Tech A*. 2014;24(5):318–322.
168. Tanaka E, Choi HS, Humblet V, Ohnishi S, Laurence RG, Frangioni JV. Real-time intraoperative assessment of the extrahepatic bile ducts in rats and pigs using invisible near-infrared fluorescent light. *Surgery*. 2008;144(1):39–48.
169. Ashitate Y, Stockdale A, Choi HS, Laurence RG, Frangioni JV. Real-time simultaneous near-infrared fluorescence imaging of bile duct and arterial anatomy. *J Surg Res*. 2012;176(1):7–13.

170. Hutteman M, Mieog JS, van der Vorst JR, et al. Intraoperative near-infrared fluorescence imaging of colorectal metastases targeting integrin alpha(v)beta(3) expression in a syngeneic rat model. *Eur J Surg Oncol*. 2011;37(3):252–257.
171. Halabi WJ, Jafari MD, Nguyen VQ, et al. Ureteral injuries in colorectal surgery: an analysis of trends, outcomes, and risk factors over a 10-year period in the United States. *Dis Colon Rectum*. 2014;57(2):179–186.
172. Schols RM, Lodewick TM, Bouvy ND, van Dam GM, Dejong CH, Stassen LP. Application of a new dye for near-infrared fluorescence laparoscopy of the ureters: demonstration in a pig model. *Dis Colon Rectum*. 2014;57(3):407–411.
173. Volonte F, Pugin F, Buchs NC, et al. Console-integrated stereoscopic OsiriX 3D volume-rendered images for da Vinci colorectal robotic surgery. *Surg Innov*. 2013;20(2):158–163.
174. Milgram P, Kishino F. A taxonomy of mixed reality visual displays. *IEICE Trans Inf Syst*. 1994;77(12):1321–1329.
175. Nicolau S, Goffin L, Soler L, eds. A low cost and accurate guidance system for laparoscopic surgery: Validation on an abdominal phantom. ACM symposium on Virtual reality software and technology; 2005.
176. Soler L, Ayache N, Nicolau S, Pennec X, Forest C, Delingette H, et al., eds. Perspectives in Image-guided Surgery. *Scientific Workshop on Medical Robotics, Navigation and Visualization (MRNV)*; 2004.
177. Soler L, Forest C, Nicolau S, Vayssiere C, Wattiez A, Marescaux J. Computer-assisted operative procedure: from preoperative planning to simulation. *Eur Clin Obstet Gynaecol*. 2006;2(4):201–208.
178. Sugimoto M, Yasuda H, Koda K, et al. Image overlay navigation by markerless surface registration in gastrointestinal, hepatobiliary and pancreatic surgery. *J Hepato-Biliary-Pancreat Sci*. 2010;17(5):629–636.
179. Volonté F, Pugin F, Bucher P, Sugimoto M, Ratib O, Morel P. Augmented reality and image overlay navigation with OsiriX in laparoscopic and robotic surgery: not only a matter of fashion. *J Hepato-Biliary-Pancreat Sci*. 2011;18:506–509.
180. Gavaghan KA, Peterhans M, Oliveira-Santos T, Weber S. A portable image overlay projection device for computer-aided open liver surgery. *IEEE Trans Biomed Eng*. 2011;58(6):1855–1864.
181. Wang M, Wu J, Lee P, et al. A landmark based registration technique for minimally invasive spinal surgery. In: *Proceedings of the 17th International Symposium on Consumer Electronics (ISCE)*. Hsinchu: IEEE, 3-6 June 2013; 235–236.
182. Gavaghan KA, Anderegg S, Peterhans M, Oliveira-santos T, Weber S. Augmented reality image overlay projection for image guided open liver ablation of metastatic liver cancer. *Augmented Environments for Computer-Assisted Interventions Lecture Notes in Computer Science*. 2012;7264:36-46.
183. Nicolau S, Soler L, Mutter D, Marescaux J. Augmented reality in laparoscopic surgical oncology. *Surg Oncol*. 2011;20(3):189–201.
184. Soler L, Nicolau S, Pessaux P, Mutter D, Marescaux J. Real-time 3D image reconstruction guidance in liver resection surgery. *Hepatobiliary Surg Nutr*. 2014;3(2):73–81.
185. Köhn A, Matsuyama R, Endo I, Schenk A. Liver surgery data and augmented reality in the operation room: experiences using a tablet device. *Int J Comput Assist Radiol Surg*. 2004;9(suppl 1):S111–S112.
186. Hayashibe M, Suzuki N, Hattori A, Otake Y, Suzuki S, Nakata N. Surgical navigation display system using volume rendering of intraoperatively scanned CT images. *Comput Aided Surg*. 2006;11(5):240–246.
187. Hayashibe M, Suzuki N, Hattori A, Otake Y, Suzuki S, Nakata N. Data-fusion display system with volume rendering of intraoperatively scanned CT images. *Int Conf Med Image Comput Comput Assist Interv*. 2005;8:559–566.
188. Birkfellner W, Figl M, Matula C, et al. Computer-enhanced stereoscopic vision in a head-mounted operating binocular. *Phys Med Biol*. 2003;48(3):N49–N57.
189. Wacker FK, Vogt S, Khamene A, et al. An augmented reality system for MR image-guided needle biopsy: initial results in a swine model. *Radiology*. 2006;238(2):497–504.
190. Fichtinger G, Deguet A, Masamune K, et al. Image overlay guidance for needle insertion in CT scanner. *IEEE Trans Biomed Eng*. 2005;52(8):1415–1424.
191. Khan MF, Dogan S, Maataoui A, et al. Navigation-based needle puncture of a cadaver using a hybrid tracking navigational system. *Invest Radiol*. 2006;41(10):713–720.
192. Khan MF, Dogan S, Maataoui A, et al. Accuracy of biopsy needle navigation using the Medarpa system—computed tomography reality superimposed on the site of intervention. *Eur Radiol*. 2005;15(11):2366–2374.
193. Schnaider M, Schwald B, Seibert H, Weller T. Medarpa—a medical augmented reality system for minimal-invasive interventions. *Stud Health Technol Inform*. 2003;94:312–314.
194. Weiss CR, Marker DR, Fischer GS, Fichtinger G, Machado AJ, Carrino JA. Augmented reality visualization using Image-Overlay for MR-guided interventions: system description, feasibility, and initial evaluation in a spine phantom. *Am J Roentgenol*. 2011;196(3):W305–W307.
195. Liao H, Inomata T, Sakuma I, Dohi T. 3-D augmented reality for MRI-guided surgery using integral videography autostereoscopic image overlay. *IEEE Trans Biomed Eng*. 2010;57(6):1476–1486.
196. Wang J, Suenaga H, Hoshi K, et al. Augmented reality navigation with automatic marker-free image registration using 3-D image overlay for dental surgery. *IEEE Trans Biomed Eng*. 2014;61(4):1295–1304.
197. Suenaga H, Hoang Tran H, Liao H, et al. Real-time in situ three-dimensional integral videography and surgical navigation using augmented reality: a pilot study. *Int J Oral Sci*. 2013;5(2):98–102.
198. Tran HH, Suenaga H, Kuwana K, et al. Augmented reality system for oral surgery using 3D auto stereoscopic visualization. *Med Image Comput Comput Assist Interv Int Conf Med Image Comput Comput Assist Interv*. 2011;14(Pt 1):81–88.
199. Fuchs H, Livingston M, Raskar R, eds. Augmented reality visualization for laparoscopic surgery. International Conference on Medical Image Computing and Computer-Assisted Intervention; 1998.
200. Mountney P, Fallert J, Nicolau S, Soler L, Mewes PW. An augmented reality framework for soft tissue surgery. *Med Image Comput Comput Assist Interv Int Conf Med Image Comput Comput Assist Interv*. 2014;17(Pt 1):423–431.
201. Figl M, Rueckert D, Hawkes D, et al. Image guidance for robotic minimally invasive coronary artery bypass. *Comput Med Imaging Graph*. 2010;34(1):61–68.

202. Su LM, Vagvolgyi BP, Agarwal R, Reiley CE, Taylor RH, Hager GD. Augmented reality during robot-assisted laparoscopic partial nephrectomy: toward real-time 3D-CT to stereoscopic video registration. *Urology*. 2009;73(4):896–900.
203. Teber D, Guven S, Simpfendorfer T, et al. Augmented reality: a new tool to improve surgical accuracy during laparoscopic partial nephrectomy? Preliminary in vitro and in vivo results. *Eur Urol*. 2009;56(2):332–338.
204. Onda S, Okamoto T, Kanehira M, et al. Identification of inferior pancreaticoduodenal artery during pancreaticoduodenectomy using augmented reality-based navigation system. *J Hepato-Biliary-Pancreat Sci*. 2014;21(4):281–287.
205. Nakamoto M, Ukimura O, Gill IS, et al. Realtime organ tracking for endoscopic augmented reality visualization using miniature wireless magnetic tracker. *Medical Imaging and Augmented Reality, 4th International Workshop*. Tokyo, Japan; August 1–2, 2008.
206. Hughes-Hallett A, Pratt P, Mayer E, et al. Intraoperative ultrasound overlay in robot-assisted partial nephrectomy: first clinical experience. *Eur Urol*. 2014;65(3):671–672.
207. Pratt P, Di Marco A, Payne C, Darzi A, Yang GZ. Intraoperative ultrasound guidance for transanal endoscopic microsurgery. *Med Image Comput Comput Assist Interv Int Conf Med Image Comput Comput Assist Interv*. 2012;15(Pt 1):463–470.
208. Hughes-Hallett A, Mayer EK, Marcus HJ, et al. Augmented reality partial nephrectomy: examining the current status and future perspectives. *Urology*. 2014;83(2):266–273.
209. Shekhar R, Dandekar O, Bhat V, et al. Live augmented reality: a new visualization method for laparoscopic surgery using continuous volumetric computed tomography. *Surg Endosc*. 2010;24(8):1976–1985.
210. Feuerstein M, Mussack T, Heining SM, Navab N. Intraoperative laparoscope augmentation for port placement and resection planning in minimally invasive liver resection. *IEEE Trans Med Imaging*. 2008;27(3):355–369.
211. Bernhardt S, Nicolau SA, Agnus V, Soler L, Doignon C, Marescaux J, eds. Automatic detection of endoscope in intraoperative CT image: *Application to AR Guidance in Laparoscopic Surgery. IEEE International Symposium on Biomedical Imaging (ISBI 2014)*.
212. Oktay O, Zhang L, Mansi T, Mountney P, Mewes P, Nicolau S, et al., eds. Biomechanically driven registration of pre- to intra-operative 3d images for laparoscopic surgery. *Medical Image Computing and Computer-Assisted Intervention—MICCAI*. Nagoya, Japan; 2013.
213. Baumhauer M, Simpfendörfer T, Müller-Stich BP, et al. Soft tissue navigation for laparoscopic partial nephrectomy. *Int J Comput Assist Radiol Surg*. 2008;3:307–314.
214. Feuerstein M, Reichl T, Vogel J, Traub J, Navab N. Magneto-optical tracking of flexible laparoscopic ultrasound: model-based online detection and correction of magnetic tracking errors. *IEEE Trans Med Imaging*. 2009;28(6):951–967.
215. Chen Y, Medioni G. Object modelling by registration of multiple range images. *Image Vision Comput*. 1992;10(3):145–155.
216. Besl PJ, McKay HD. A method for registration of 3-D shapes. *IEEE Trans Pattern Anal Mach Intell*. 1992;14(2):239–256.
217. Dickfeld T, Lei P, Dilsizian V, et al. Integration of three-dimensional scar maps for ventricular tachycardia ablation with positron emission tomography-computed tomography. *JACC Cardiovasc Imaging*. 2008;1(1):73–82.
218. Bertaglia E, Bella PD, Tondo C, et al. Image integration increases efficacy of paroxysmal atrial fibrillation catheter ablation: results from the CartoMerge Italian Registry. *Europace*. 2009;11(8):1004–1010.
219. Caponi D, Corleto A, Scaglione M, et al. Ablation of atrial fibrillation: does the addition of three-dimensional magnetic resonance imaging of the left atrium to electroanatomic mapping improve the clinical outcome?: a randomized comparison of Carto-Merge vs. Carto-XP three-dimensional mapping ablation in patients with paroxysmal and persistent atrial fibrillation. *Europace*. 2010;12(8):1098–1104.
220. Maier-Hein L, Mountney P, Bartoli A, et al. Optical techniques for 3D surface reconstruction in computer-assisted laparoscopic surgery. *Med Image Anal*. 2013;17(8):974–996.
221. Rohl S, Bodenstedt S, Suwelack S, et al. Dense GPU-enhanced surface reconstruction from stereo endoscopic images for intraoperative registration. *Med Phys*. 2012;39(3):1632–1645.
222. Lee SL, Lerotic M, Vitiello V, et al. From medical images to minimally invasive intervention: Computer assistance for robotic surgery. *Comput Med Imaging Graph*. 2010;34(1):33–45.
223. Stoyanov D, Scarzanella MV, Pratt P, Yang GZ. Real-time stereo reconstruction in robotically assisted minimally invasive surgery. *Med Image Comput Comput Assist Interv Int Conf Med Image Comput Comput Assist Interv*. 2010;13(Pt 1):275–282.
224. Mountney P. Three-dimensional tissue deformation recovery and tracking. *IEEE Signal Process Mag*. 2010;27:14–24.
225. Hu M, Penney G, Figl M, et al. Reconstruction of a 3D surface from video that is robust to missing data and outliers: application to minimally invasive surgery using stereo and mono endoscopes. *Med Image Anal*. 2012;16(3):597–611.
226. Garcia-Grasa O, Bernal E, Casado S, Gil I, Montiel J. Visual SLAM for hand-held monocular endoscope. *IEEE Trans Med Imaging*. 2014;33(1):135–146.
227. Mountney P, Yang G-Z, eds. Motion compensated SLAM for image guided surgery. *International Conference on Medical Image Computing and Computer-Assisted Intervention*; 2010.
228. Mahmoud N, Nicolau SA, Keshk A, Ahmad MA, Soler L, Marescaux J, eds. *Fast 3D Structure From Motion with Missing Points from Registration of Partial Reconstructions International Conference on Articulated Motion and Deformable Objects (AMDO'12)*; 2012.
229. Okatani T, Deguchi K. Shape reconstruction from an endoscope image by shape from shading technique for a point light source at the projection center. *Comput Vis Image Underst*. 1997;66(2):119–131.
230. Quartucci CH, Tozzi CL, eds Towards 3D Reconstruction of Endoscope Images using Shape from Shading. In: *Proceedings of the 13th Brazilian Symposium on Computer Graphics and Image Processing*; 2000.

231. Collins T, Pizarro D, Bartoli A, Canis M, Bourdel N, eds. Computer-assisted laparoscopic myomectomy by augmenting the uterus with pre-operative MRI data. *IEEE International Symposium on Mixed and Augmented Reality (ISMAR 2014)*; 2014.
232. Malti A, Bartoli A. Combining conformal deformation and Cook-Torrance shading for 3-D reconstruction in laparoscopy. *IEEE Trans Biomed Eng*. 2014;61(6):1684–1692.
233. Penne J, Holler K, Sturmer M, et al. Time-of-Flight 3-D endoscopy. *Med Image Comput Comput Assist Interv Int Conf Med Image Comput Comput Assist Interv*. 2009;12(Pt 1):467–474.
234. Mourgues F, Vieville T, Falk V, Coste-Manière E, editors. Interactive Guidance by Image Overlay in Robot Assisted Coronary Artery Bypass. Medical Image Computing and Computer-Assisted Intervention—MICCAI 2003. Montréal, Canada: Springer Berlin, Heidelberg; 2003.
235. Puerto-Souza GA, Mariottini GL. A fast and accurate feature-matching algorithm for minimally-invasive endoscopic images. *IEEE Trans Med Imaging*. 2013;32(7):1201–1214.
236. Puerto-Souza GA, Cadeddu JA, Mariottini GL. Toward long-term and accurate augmented-reality for monocular endoscopic videos. *IEEE Trans Biomed Eng*. 2014;61(10):2609–2620.
237. Bookstein F. Principal warps: thin-plate splines and the decomposition of deformations. *IEEE Trans Pattern Anal Mach Intell*. 1989;11:567–585.
238. Rueckert D, Sonoda LI, Hayes C, Hill DL, Leach MO, Hawkes DJ. Nonrigid registration using free-form deformations: application to breast MR images. *IEEE Trans Med Imaging*. 1999;18(8):712–721.
239. Tsai Y, Lin H, Hu Y. Thin-plate spline technique for medical image deformation. *J Med Biol Eng*. 2000;20(4):203–210.
240. Cash DM, Miga MI, Sinha TK, Galloway RL, Chapman WC. Compensating for intraoperative soft-tissue deformations using incomplete surface data and finite elements. *IEEE Trans Med Imaging*. 2005;24(11):1479–1491.
241. Bano J, Hostettler A, Nicolau SA, Cotin S, Doignon C, Wu HS, et al.,editors. Simulation of Pneumoperitoneum for Laparoscopic Surgery Planning. Medical Image Computing and Computer-Assisted Intervention—MICCAI; 2012.
242. Registration of preoperative liver model for laparoscopic surgery from intraoperative 3D acquisition. In: Bano J, Nicolau SA, Hostettler A, Doignon C, Marescaux J, Soler L, editors. *Augmented Reality Environments for Medical Imaging and Computer-Assisted Interventions*. Japan: Nagoya; 2013.
243. Heizmann O, Zidowitz S, Bourquain H, et al. Assessment of intraoperative liver deformation during hepatic resection: prospective clinical study. *World J Surg*. 2010;34(8):1887–1893.
244. Sanchez-Margallo FM, Moyano-Cuevas JL, Latorre R, et al. Anatomical changes due to pneumoperitoneum analyzed by MRI: an experimental study in pigs. *Surg Radiol Anat*. 2011;33(5):389–396.
245. Zijlmans M, Langø T, Hofstad EF, Van Swol CF, Rethy A. Navigated laparoscopy—liver shift and deformation due to pneumoperitoneum in an animal model. *Minim Invasive Ther Allied Technol*. 2012;21(3):241–248.
246. Hostettler A, George D, Remond Y, Nicolau SA, Soler L, Marescaux J. Bulk modulus and volume variation measurement of the liver and the kidneys in vivo using abdominal kinetics during free breathing. *Comput Methods Programs Biomed*. 2010;100(2):149–157.
247. Ribes D, Peterhans M, Anderegg S, Banz V, Candinas D, Weber S. Towards higher precision in instrument guided liver surgery: automatic registration of 3D ultrasound with pre-operative MeVis-CT. *Int J Comput Assist Radiol Surg*. 2012;7(1S):141–145.
248. Dumpuri P, Clements LW, Dawant BM, Miga MI. Model-updated image-guided liver surgery: preliminary results using surface characterization. *Prog Biophys Mol Biol*. 2010;103:197–207.
249. Kingham TP, Scherer MA, Neese BW, Clements LW, Stefansic JD, Jarnagin WR. Image-guided liver surgery: intraoperative projection of computed tomography images utilizing tracked ultrasound. *HPB (Oxford)*. 2012;14(9):594–603.
250. Hansen C, Wieferich J, Ritter F, Rieder C, Peitgen HO. Illustrative visualization of 3D planning models for augmented reality in liver surgery. *Int J Comput Assist Radiol Surg*. 2010;5(2):133–141.
251. Virtual reality and augmented reality applied to endoscopic and notes procedures. In: Soler L, Nicolau S, Hostettler A, Fasquel J, Agnus V, Charnoz A, et al.,editors. *World Congress on Medical Physics and Biomedical Engineering*. Munich, Germany: Springer; 2009.
252. Azagury DE, Ryou M, Shaikh SN, et al. Real-time computed tomography-based augmented reality for natural orifice transluminal endoscopic surgery navigation. *Br J Surg*. 2012;99(9):1246–1253.